Master's thesis

NTNU
Norwegian University of Science and Technology
Faculty of Information Technology and Electrical Engineering
Department of Engineering Cybernetics

Sondre Mosnes Heimvik

Energy optimized navigation in drones

Master's thesis in Industrial Cybernetics
Supervisor: Morten Dinhoff Pedersen
January 2024

NTNU
Norwegian University of
Science and Technology

Sondre Mosnes Heimvik

Energy optimized navigation in drones

Master's thesis in Industrial Cybernetics
Supervisor: Morten Dinhoff Pedersen
January 2024

Norwegian University of Science and Technology
Faculty of Information Technology and Electrical Engineering
Department of Engineering Cybernetics

Sammendrag

Denne avhandlingen ble skrevet med mål om å undersøke forholdet mellom masse, kraft og energiforbruk. For å få innsikt i forholdet mellom dem, ble ble det inkludert informasjon med formål om å gi forståelse av UAV-flygning, både med hensyn til regelverket som styrer disse operasjonene i Norge, men også med hensyn til bevegelsene til et quadcopter gjennom luften. Dette ble oppnådd ved inkludering av informasjon om quadcopter-kinetikk og kinematikk, der den kinetiske modellen beskriver effekten av krefter og dreiemomenter, og den kinematiske modellen beskriver quadcopterbevegelsen uten inkludering av krefter og dreiemomenter. Slik ble det oppnådd forstelse rundt den konstante likevekten som er oppnådd mellom krefter og dreiemomenter under reise med konstant hastighet, hilket er fundamentalt for denne modellen.

Deretter ble det funnet en modell for strømforbruk ved å bruke kunnskap fra Årsandøy og andre for å integrere masse i en allerede nyttig modell. De individuelle strømtapene ble forklart og formulert som funksjoner av masse og reisehastighet, for å få en fullstendig modell av de totale strømtapene som oppstår under flyging. I tillegg til dette ble det inkludert uttrykk for strømtapene for individuelle lineære bevegelser som oppover, nedover og bortover flygning, samt. sveving.

For å få forståelse for sammenhengen UAV-operasjoner skjer i og reguleringene rundt emnet, ble reguleringene begrenset til de som gjelder i Norge, for å opprettholde realisme og relevans. De ulike operasjonstypene og lisens-typene ble beskrevet. Disse ble også inkludert fordi reguleringene kan vise seg å være nødvendige for et eventuelt optimeringsproblem. Denne typen optimeringsproblem ble skissert og anvendt på tre forskjellige case-studier.

Resultatene fra studiene ble brukt til å undersøke validiteten til modellen, forholdet mellom optimal hastighet og masse, og forholdet mellom masse og energiforbruk per avstandsenhet. Det ble funnet at modellen produserte resultater som var relativt like som forventet, og at masse oppfører seg nesten som en skaleringsfaktor for strømforbruket.

I fremtiden ville det være gunstig å gjøre mer testing av modellen i forskjellige scenarier, og implementere forbedringer i tilgjengeligheten av testdata for forskjellige UAV-modeller.

Abstract

This thesis was written with the objective of examining the relationship between mass and power and energy consumption. In order to gain insight into the relationship between them, information was provided that was aimed to at providing an understanding of the intricacies of UAV flight, both with regards to the regulations which govern these operations in Norway, but also with regards to the movements of a quadcopter in flight. This was accomplished through inclusion of information on quadcopter kinetics and kinematics, where the kinetic model describes the effect of forces and torques, and the kinematic model describes quadcopter movement without inclusion of forces and torques. Through this, it was explained how the equilibrium that is present between the forces and torques affecting the UAV is essential to this model.

Next, a power consumption model was found, using knowledge gained from Årsandøy as well as others to incorporate mass into an already useful model. The individual power losses were explained and formulated as functions of mass and travel speed, in order to gain a complete model of the total power losses experienced during flight. In addition to this, these were used to express the power losses of individual linear movements like ascent, descent, horizontal flight and hovering.

In order to gain an understanding about the context in which UAV operations happen, and the regulations surrounding the topic. The regulations were limited to the one applicable in Norway in order to maintain realism and relevance. The different operation types and licenses were described. These were also included because the regulations might prove to be essential as constraints for an eventual optimization problem. This type of optimization problem was outlined and applied to three different case studies.

The results from the studies were used to examine the viability of the model, the relationship between optimal speed and mass, and the relationship between mass and energy consumption per distance unit. It was found that the model produced results that were in line with expected patterns, and that mass behaves almost like a scaling factor for power consumption.

In the future, it would be beneficial to do more testing of the model in different scenarios and implement improvements in the availability of test data for different UAV models.

Preface

This master's thesis is submitted as part of the subject TTK4900 - Engineering Cybernetics, Master's Thesis worth 30 credits. It is submitted as part of the requirements of the 2-year masters programme Industrial Cybernetics, at the Norwegian University of Science and Technology (NTNU). The research done as part of this thesis has proven to be incredibly challenging, but also interesting. My work on this thesis has provided me with useful experiences with research, and have helped me manage how i approach new challenges.

Sondre Mosnes Heimvik January 22nd 2024

Acknowledgements

During my work on this thesis, the support from my family and my girlfriend have been integral in keeping me going. They have assisted in making dinners for me, cleaning and just being incredibly supportive emotionally. I would also like to thank my supervisor Morten Dihoff Pedersen for accepting my request to write a master's thesis well outside the normal writing term, letting me write even in spite of some issues arising with my study points, and in general being one of the best professors i have ever had. The only thing i regret is not making more contact with him during my work on this thesis.

Table of Contents

List of Figures

List of Tables

Nomenclature

RPAS	This is a term which describes the aircraft itself along with the ground control station, telemetry and communications systems, launch and landing equipment, sensors and other hardware and software used to operate the aircraft.
RO	RPAS operator
SORA	Specific operation risk assessment
PDRA	Pre-defined risk assessment
STS	Standard scenario
LUC	Light UAS operator certificate
VLOS	Visual line of sight
AGL	Above ground level
HTA	Heavier than air
LTA	Lighter than air
BCR	Battery consumption rate
DOF	Degrees of freedom
CG	Center of Gravity
CO	Coordinate origin
ConOps	Concept of Operation
BVLOS	Beyond visual line of sight
OSO	Operational Safety Objective
SAIL	Specific Assurance Integrity Level
UAV	Unmanned aerial vehicle

1 Introduction

Since being legalized in 2006 [4], the market for Non-military Unmanned Aerial Vehicles(UAV), colloquially known as drones, has seen a meteoric increase in value [51]. Drones entered the market with promises of environmentally beneficial, scalable and cost effective operation. They also came with the promise of increased ease of access in operations in tight spaces, and reduced risk to humans in applications where it might be dangerous for a human to go [18]. Since first being introduced, drones have seen use in a myriad of use cases, some among them being search and rescue, terrain mapping, photography, bridge inspection and package delivery.

Many of these can be performed with highest efficiency using drone automation, however there are several factors restricting the current capabilities of autonomous drone missions. When using lighter-than-air UAVs, the most important obstacle is the lack of control over the UAV due to atmospheric interference. In order to overcome this, heavier-than-air (HTA) UAVs are more commonly used in the aforementioned use cases. The largest obstacle when using heavier-than-air (LTA) UAVs is the constant energy consumption required to maintain flight, as there is a finite amount of energy available in the UAVs batteries. There are also restrictions imposed on UAV missions by governing bodies of the world in order to carry out missions in a safe and structured way that avoids interference with other air traffic. Planning missions require determining an optimal route for the UAV to follow.

A framework was set forth by Finn Matras and Morten Pedersen in their 2023 paper[42], which describes a model which can be used to accurately simulate a quadcopter heavier than air unmanned aerial vehicle (UAV) without using computationally intensive fluid dynamics (CFD) analysis [10]. It was showcased in her thesis that the model can be implemented for a theoretical energy efficiency improvement, and that the model set forth by Matras and Pedersen is relatively accurate in most cases.

The objective of this thesis is to utilize the works of Årsandøy, and by extension Matras and Pedersen, to expand on the results of her thesis by examining the relationship between payload weight and power consumption of a UAV. In this thesis, the scope will be limited to quadcopter UAVs. Further, an attempt will be made to utilize the results to aid in optimization of flight plans for UAVs.

1.1 Objectives

Because energy usage is such an important factor in LTA UAV missions, the objective of this research was to utilize and build upon the knowledge gained from the work of Frida [10] to achieve savings in energy usage by examining energy usage as a function of payload weight. Thus, the objective can be summarized in two points:

· minimize energy usage

· maximize flight distance

This would have to be done through optimization of flight paths. It is also necessary to adapt the results to any legislation that regulate UAV usage. The end goal is to find ways to utilize this

research in real world scenarios where UAVs can be utilized. The focus will be on minimization of energy usage regardless of laws, as it is more generally applicable, and less subject to change than the same scenarios would be with the consideration of laws.

1.2 Research agenda

In order to be able to reach the desired outcome from the research done on this thesis, the time allotted was divided into a few key points:

· Finding a model that describes the relationship between drone movements, payload weight and energy usage

· Identifying relevant case studies that are relevant to realistic scenarios

· Parameter identification and model validation

· Optimization of energy consumption of an example drone

1.3 Motivation

The objectives of the thesis can be formulated as an optimization problem. The optimization problem utilizes the power consumption equation for the drone as cost function to be minimized. The most widely applicable constraints stem from the physics of multicopter flight, in which a constant equilibrium of forces is required in order to maintain steady state flight. This is the core principle of multicopter flight. Based on parameters such as mass, motor type, propeller type, size and configuration, the amount of thrust required to maintain this equilibrium changes. This is also a deciding factor in determining the angle of attack that the multicopter is able to maintain during flight. Thus, the optimization problem must include constraints such as:

- Constraints on the flight angle of the copter
- A constraint enforcing equilibrium of forces
- Constraints on maximum power consumption and thrust

In order to comply with local regulations, they will also have to be implemented as constraints. These are usually determined by authorities like the European Union Aviation Safety Administration(EASA) in Europe or the Federal Aviation Administration(FAA) in the USA, and are often implemented into local regulation as well. The exact laws depend on the nature of the UAV operations, but typically include limitations on

- Maximum velocity
- Maximum altitude
- Area of operations

Because regulatory constraints typically come in the form of minimum and maximum values for a given parameter, they will be implemented as inequality constraints. Some constraints such as

maximum velocity might appear both in drone datasheets and in regulatory constraints, in which case the regulations will always be prioritised.

1.4 Outline

This section is meant to provide an overview of the structure of this thesis. It contains surface level information on what information is included in each chapter.

Chapter 1 - Introduction

This is an introductory chapter meant to explain the fundamentals of the problem and the background of the objective of this thesis. The contents are meant to give insight into the objectives of the thesis and the way the research was executed in order to achieve them. It contains some info about the different types of UAVs that exist, and defines the types that are relevant to this thesis. The contents of the chapter are also meant to include the limitations placed on a quadcopter UAV, both due to the physics of the drone and the regulations in the area in which it is used. Next, an overview of the motivation of the problem, including the relationship between the different constraints and their origins. The outline of the thesis is provided, before vital previous work in the field of UAV power management is detailed. Lastly, contributions from this thesis will be listed.

Chapter 2 - Modeling

This chapter provides detailed explanation of the drag forces affecting a quadcopter UAV during flight. It also provides valuable insight into the modeling of a UAV for use in digital simulations, including information on the kinetics and kinematics of the UAV and the coordinate systems used in the model. In order to create an understanding of the movements of a quadcopter, a breakdown of the forces acting on the UAV and the equilibrium it's in during flight is included.

Chapter 3 - Power consumption

Causes of power consumption are detailed, which provides the fundamentals of the power consumption model. Along with the physical origins of the power losses experienced by the system, information regarding their connection to the the forces mentioned in chapter 2 is provided.

Chapter 5 - Optimization problem

The information from chapters 2 and 3 is used to construct an optimization problem, with the objective being minimization of power consumption, constrained by the physical limitation of drone movement and regulatory bodies of the area of operation.

Chapter 6 - Case studies

An attempt is made to construct case studies in which the model developed earlier can be utilized. Each of the case studies are aimed at constructing scenarios that each showcase use cases for the model. The objective of this chapter is to demonstrate the ability to implement the model to predict real life UAV behaviour, and to observe the real life effects of varying constraints without needing to carry out physical testing. The case studies can also provide some insight into what kind of drone movements are best for efficiency, and which limitations are the most prominent in real life use cases.

Chapter 7 - Parameter identification and model validation

This chapter contains the procedure for identifying the parameters required for the model found in chapter 5. It includes examples of finding the parameters for a few different UAV models. These parameters are pulled from several different sources in order to showcase multiple ways of acquiring the desired values.

Chapter 8 - Results

This chapter presents the results and findings from the previous chapters, and contains discussion around the validity of the model, upsides and downsides found, and other observations made during simulation.

Chapter 9 - Conclusion

The conclusion contains a short summary of what has been discussed in this thesis and the results found in chapter 8. It also contains some suggestions for future work to be done to further build upon the knowledge gained in this report.

1.5 Power requirements

Power is defined as "[the]time rate of doing work or delivering energy, expressible as the amount of work done, or energy transferred, divided by the time interval"[16]. As such, the power of a drone is the energy usage per time unit. The drag force affecting any given part of the drone is responsible for about 95% of the power consumption [30], generally increases with increasing velocity of that part. Since drag forces cause the overwhelming majority of the power losses on a drone, examining the losses due to drag is deemed sufficient for creating a model, and is likely to result in relatively high accuracy. The drag forces affecting a quadcopter during flight are parasitic drag, profile drag and induced drag. Induced drag and parasitic drag affect the quadcopter's chassis, while the profile drag is a force affecting the blades of the rotors. Parasite drag Increases with increasing drone velocity, while induced drag decreases with increasing drone velocity. The relationship between these forces and velocity means there's a velocity in which the total drag affecting the drone chassis is minimized. This can be illustrated as shown in figure 1.

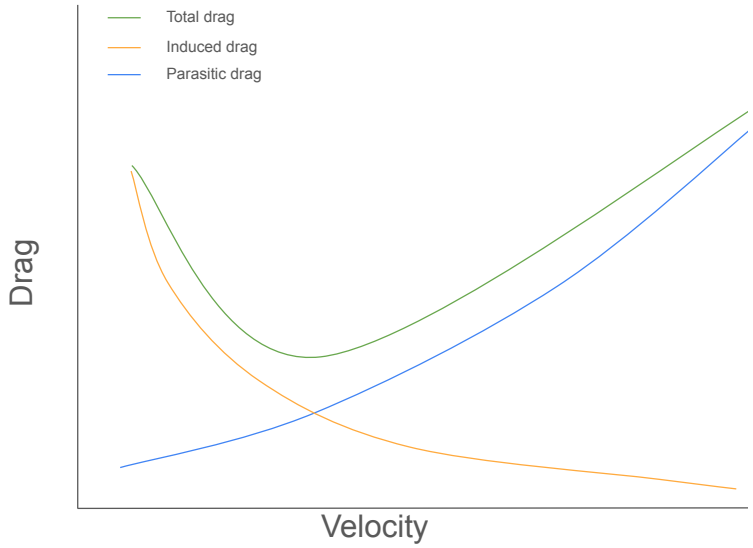

Figure 1: A sketch showing the general trends of parasite-, induced-, and total drag with increasing velocity

Parasitic drag

Parasitic drag is comprised of form drag, friction drag and interference drag [41]. Form drag is the resistance caused by the separation of a boundary layer from a surface, and the wake it creates. When multiple geometries are joined together, the space for air to flow around the join is restricted, leading to turbulent mixing of the airflows around each shape. This is known as interference drag. Friction drag is related to the roughness of the surface of the UAV and increases with rougher surfaces. This is caused by increased thickness of the boundary layer of the fluid around the UAV. These drag force increases with increasing velocity. Parasite power is defined as the power required in order to overcome the parasite drag force, meaning the drag force around the non lift-generating parts of the UAV. As the components of this force all increase with increasing velocity, so does the parasite power. The parasitic drag force is proportional to the square of the velocity of the body it's acting on, and the profile power is proportional to the cube of the same velocity.

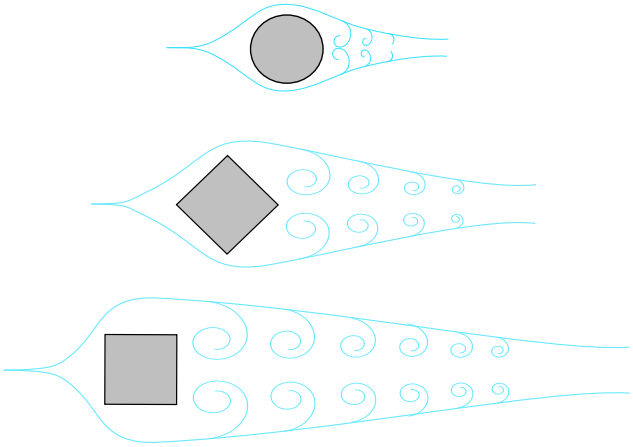

Figure 2: A sketch showing the parasite drag for different geometries [19]

Profile drag

Profile drag is a drag force created by the rotating fan blades as they impact the air in front of them. It is a force that can be viewed as a parasite drag that is specific to lift-generating parts of a UAV. The drag force generated is parallel to the fluid flow around the propeller blade. While the parasite power can be equal to zero during hover, profile power is a direct consequence of the rotation of the rotor blades, meaning that it is non-zero for as long as the drone motors are powered.

Induced drag

Induced drag is a force that affects lift-generating parts of HTA aircraft, meaning it affects wings of a fixed wing aircraft and the rotors of a quadcopter. It is a drag force that is caused by wing tip vortices created because of the pressure difference between the top and bottom of the rotor blade [24]. These vortices are turbulent in nature, and thus cause a drag force. Because the pressure differences above and below the wings or rotor blades are necessary for lift generation, the generation of this drag force is an unavoidable byproduct of lift generation. The induced power is defined as the power required to overcome the induced drag force. At low aircaft velocities, these power requirements are a substantial part of the total. However, during forward flight, it is clear that parasite power requirements increase quicker and become dominant at higher speeds.

1.6 Previous work

As limited battery capacity is one of the most significant obstacles to more widespread UAV application, various efforts have been made to improve the power consumption of the available UAVs today. These efforts span multiple disciplines and include improvements to, among others, the following aspects of UAVs:

- Developing a model which aims to optimize power consumption by examining the relationship

between travel speed and power consumption [10].

- Improving the aerodynamics by optimising drone geometry [31].
- Wireless battery charging to facilitate automation and extended missions [35].

While a fair amount of work has been done to reduce power consumption, little research was found that focused on examining the relationship between drone movement and mass, while also taking regulation into account. There is work done to explore optimization of drone flight paths, such as by A. Bahabry et.al. [13], however these efforts seem more focused on large networks of drones. Quite a bit of work has also been done to improve upon drone navigation utilizing sensors, such as the work done by Moskalenko et al [34]. It is worth noting that there are articles tackling the impact of payload on energy consumption. One such example is a paper by Torabbeigi, Lim & Kim [46]. In their paper, they provide detailed information on Battery Consumption Rate (BCR) in the context of scheduling and use of multiple drones during delivery. They go over the planning required to perform missions using such a setup, develop an algorithm to process the variable in their model and use these to arrive at numerical solutions for a given drone. They found a linear correlation between BCR and payload amount. They also found that up to 60% of the simulated flight paths failed when not accounting for BCR. Another paper of note was written by Abeywickrama, Jayawickrama, He & Dutkiewicz [2]. In the paper, they provide detailed insight into the power consumption of a quadcopter, both on the ground and in the air. They also expand on the power consumption during aerial movement, and develop a model for the power consumption. It should be noted that their model is based on linear regression, mostly resulting in linear models for energy usage. They conclude that this model is accurate and efficient enough for use in energy calculations for UAV mission, and intend to use it in their own research. The final Paper that should be mentioned is written by Liu, Sengupta & Kurzhanskiy [30], and contains a comprehensive model which includes both different isolated movements and incorporation of mass. This model is based entirely on theory, and is thus mathematically quite different from the one found in [2]. They proceed to validate the model by performing their own validation experiments. They conclude that the model they developed is fairly accurate, and that the next step in improving it is to estimate wind speeds. None of these papers implement mass, movements and regulations, and thus do not give a complete picture of realistic operation. they also do not take into account available energy and different drone configurations. These will therefore be included in this report.

1.7 Contributions

By the time this thesis is finished, the following contributions will be made:

- Provide insight into the energy consumption of quadcopters
- Examine the energy consumption for a single drone for isolated movement
- Examine the relationship between mass and power consumption
- Provide some realistic scenarios where this knowledge can be applied
- Develop some insight into how quadcopters should move to conserve energy

2 Modeling

In order to understand the movements of a multicopter UAV, a model is developed. This model consists of a kinematic description of UAV movements, and a description of the kinetics of the UAV. Modeling the kinematics of a UAV is a way of describing its movements without regard to the forces and torques affecting it. The aim of the model is purely to provide description of the spatial position of the UAV [15]. Because the kinematic model doesn't include the forces affecting the UAV, a kinetic model is developed for the purpose of describing the forces and torques affecting the UAV. It is common that a process called control allocation is employed after developing these models, as it simplifies the control of the UAV through consolidation of multiple inputs into one, thus reducing the computational requirements needed for UAV operation.

2.1 Coordinate frames

In order to be able to model and program a quadcopter, the position and orientation of the copter is given in two different coordinate frames, a fixed frame which is aligned with the quadcopter body and an inertial frame which is centered in a stationary point on the ground. The fixed body frame has its Coordinate Origin (CO) placed in its center of gravity (CG), and the quadcopter is considered symmetric along all three axes. The quadcopter is assumed to be perfectly balanced around the center of the hub, with the arms length, arm mass and rotor mass all being equal for each rotor. Following this, the CG and CO of the fixed body frame are placed in the center of the hub, with x_b being aligned with the "forward facing" arm, y_b being aligned with the left arm and z_b being perpendicular to x_b and y_b, facing directly upward. This is shown in figure 3. The inertial frame is considered stationary relative to the earth.

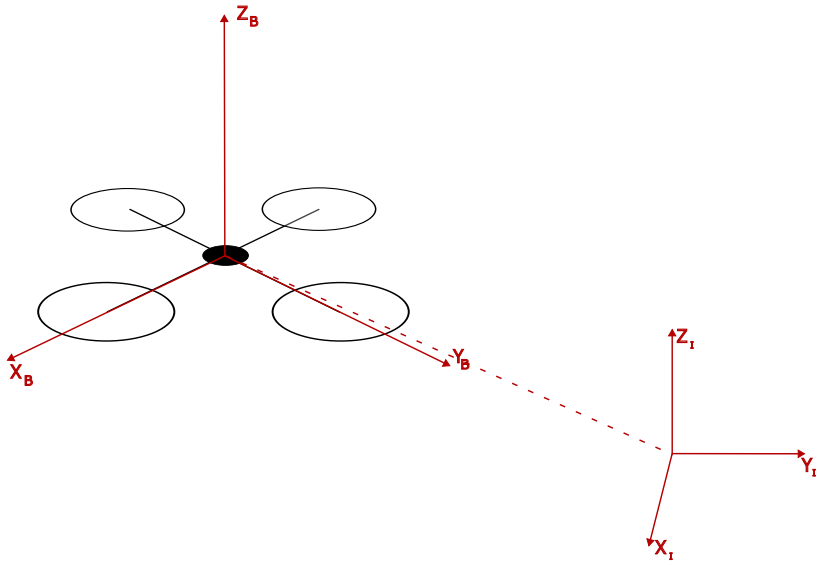

Figure 3: A sketch showing the body- and inertia-coordinate frames.

2.2 Kinematics

The drone is modeled as a rigid body with 6 degrees of freedom (DOF), three of which are rotational and three are linear. In order to represent this mathematically, the vectors η and ν are defined as shown in equations 1.

$$\eta = \begin{bmatrix} x \\ y \\ z \\ \phi \\ \theta \\ \psi \end{bmatrix} \nu = \begin{bmatrix} u \\ v \\ w \\ p \\ q \\ r \end{bmatrix} \tag{1}$$

The ν vector contains linear and rotational velocities. In order to simplify the research and calculations done in relation to this topic, only linear movements and non-rotational states will be considered. As such, the rotational velocities in the body frame will be disregarded, and the ν is simplified, resulting in the vector shown in 2.

$$\nu = \begin{bmatrix} u \\ v \\ w \\ 0 \\ 0 \\ 0 \end{bmatrix} \tag{2}$$

In order to perform simulations using this model, the rigid body frame and the inertial frame must be connected. This is done using translation and rotation matrices, which translate between the respective frame coordinates. The rotation matrix describes the rotation necessary to align the coordinate frames, while the translation matrix describes the necessary movements for alignment of the coordinate origins of the frames. The rotation and translation matrices required to describe a multicopter UAV are given in [8], and are displayed below in equations 3 and 4 respectively.

$$R_b^i = \begin{bmatrix} C_\psi C_\theta & C_\psi S_\theta S_\phi - S_\psi C_\phi & C_\psi S_\theta C_\phi + S_\psi S_\phi \\ S_\psi C_\theta & S_\psi S_\theta S_\phi + C_\psi C_\phi & S_\psi S_\theta C_\phi - C_\psi S_\phi \\ -S_\theta & C_\theta S_\phi & C_\theta C_\phi \end{bmatrix} \tag{3}$$

$$T_b^i = \begin{bmatrix} 1 & S_\phi t_\theta & C_\phi t_\theta \\ 0 & C_\phi & -S_\phi \\ 0 & \frac{C_\phi}{C_\theta} & \frac{C_\phi}{C_\theta} \end{bmatrix} \tag{4}$$

where

- $S_i = \sin(\text{i})$
- $C_i = \cos(\text{i})$
- $t_i = \tan(\text{i})$

The R- and T-matrices can be concatenated along with two 3x3 zero-matrices to form the matrix $J(\eta)$ as shown in equation 5. Using this matrix, the kinematics of this model can be expressed as shown in equation 6 [10].

$$J(\eta) = \begin{bmatrix} R_b^i & 0_{3\times3} \\ 0_{3\times3} & T_b^i \end{bmatrix} \tag{5}$$

$$\dot{\eta} = J(\eta)\nu \tag{6}$$

2.3 Kinetics

The kinetics of the UAV are a mathematical expression of the forces and torques acting upon the UAV. The kinetics of the drone are described by equation 7 [28]. It can be reworked to express $\dot{\nu}$ as a function of ν, as shown in equation 8.

$$M\dot{\nu} + C(\nu)\nu = \tau(\nu) \tag{7}$$

$$\dot{\nu} = M^{-1}(\tau(\nu) - C(\nu)\nu) \tag{8}$$

The equation consists of the global system inertia matrix M, the coriolis matrix C, and the vector τ, which contains the generalized forces and moments [21].

$$C_\nu = \begin{bmatrix} 0 & 0 & 0 & m(y_g q + z_g r) & -m(x_g q - \omega) & -m(x_g r + v) \\ 0 & 0 & 0 & -m(y_g p + \omega) & m(z_g r + x_g p) & -m(y_g r - u) \\ 0 & 0 & 0 & -m(z_g p - v) & -m(z_g q + u) & m(x_g p + y_g q) \\ -m(y_g q + z_g r) & m(y_g p + \omega) & m(z_g p - v) & 0 & -I_{yz}q - I_{xz}p + Izr & Iyzr + I_{xy}p - I_y q \\ m(x_g q - \omega) & -m(z_g r + x_g p) & m(z_g q + u) & I_{yz}q + I_{xz}p - I_z r & 0 & -I_{xz}r - I_{xy}q + I_x p \\ m(x_g r + v) & m(y_g r - u) & -m(x_g p + y_g q) & -I_{yz}r - I_{xy}p + I_y q & I_{xz}r + I_{xy}q - I_x p & 0 \end{bmatrix} \tag{9}$$

For a quadcopter that has CO in the CG and is symmetric about all three axes, an inertial matrix I is given by equation 10 [22]. In the J-matrix, it can be observed that all values not on the diagonal are equal to zero. It is also stated that the inertial matrix shown in 10 is valid only when the CG is in the CO, meaning $[x_g, y_g, z_g] = [0, 0, 0]$. This can be used to formulate a simplified Coriolis matrix shown in equation 11.

$$I = \begin{bmatrix} I_{xx} & 0 & 0 \\ 0 & I_{yy} & 0 \\ 0 & 0 & I_{zz} \end{bmatrix} \tag{10}$$

Using the simplified inertia matrix, the coriolis matrix can also be simplified, resulting in the coriolis matrix shown in equation 11.

$$C_\nu = \begin{bmatrix} 0 & 0 & 0 & 0 & m\omega & -mv \\ 0 & 0 & 0 & -m\omega & 0 & mu \\ 0 & 0 & 0 & mv & -mu & 0 \\ 0 & -m\omega & mv & 0 & I_z r & -I_y q \\ m\omega & 0 & -mu & -I_z r & 0 & I_x p \\ -mv & mu & 0 & I_y q & -I_x p & 0 \end{bmatrix} \tag{11}$$

The remaining components required in order to express $\dot{\nu}$ through equation 8 are the system inertia matrix M and the torque vector τ. This matrix consists of four sub-matrices, where $M_{1,1} = mI_{3x3}$ and $M_{2,2} = I$. It is important to note that the matrix I is the simplified inertia matrix, while the matrix I_{3x3} is a 3x3 identity matrix. The remaining sub-matrices are 3x3-matrices containing only zeros. As such, the M-matrix is given by equation 12 [10].

$$M = \begin{bmatrix} m & 0 & 0 & 0 & mz_g & -my_g \\ 0 & m & 0 & -mz_g & 0 & mx_g \\ 0 & 0 & m & my_g & -mx_g & 0 \\ 0 & -mz_g & my_g & I_{xx} & -I_{xy} & I_{xz} \\ mz_g & 0 & -mx_g & -I_{yx} & I_{yy} & -I_{yz} \\ -my_g & mx_g & 0 & -I_{zx} & -I_{zy} & I_{zz} \end{bmatrix} = \begin{bmatrix} m & 0 & 0 & 0 & 0 & 0 \\ 0 & m & 0 & 0 & 0 & 0 \\ 0 & 0 & m & 0 & 0 & 0 \\ 0 & 0 & 0 & I_{xx} & 0 & 0 \\ 0 & 0 & 0 & 0 & I_{yy} & 0 \\ 0 & 0 & 0 & 0 & 0 & I_{zz} \end{bmatrix} \tag{12}$$

The force- and torque vector must also be determined in order to complete the kinetic model for the quadcopter. The forces and torques included in the vector are caused by the propeller τ_{prop}, by gravity τ_g [10], and by the resistance of a rigid body moving through a fluid τ_{res} [33]. In Matras' paper from 2020 [33], it is stated that the total drag can be mathematically formulated as

$$\tau_{tot}(\nu) = \tau_{act}(\nu, u) - \tau_g(\eta) - \tau_{res}(\nu) \tag{13}$$

The actuator torque τ_{act} is caused by the movement of the rotors. It is directly related to the angular velocity of the propeller, and is assumed to act strictly along the z-axis [10]. In the following equation, n is the number of rotors on the UAV, and ω is the angular velocity of a given rotor, denoted by the index i.

$$\tau_{act}(\nu, u) = \sum_{i=1}^{n} \tau_i \tag{14}$$

The gravity force is denoted as τ_g, and is a force acting on the UAV, pointing to the ground. It is described in equation 15, in which m is the UAV mass including payload and g is the gravitational acceleration of earth. The angles θ and ϕ describe the rotation of the UAV.

$$\tau_g(\eta) = \begin{bmatrix} mgsin\theta \\ -mgcos\theta sin\phi \\ -mgcos\theta cos\phi \\ 0 \\ 0 \\ 0 \end{bmatrix} \tag{15}$$

The resistance caused by movement through a fluid is expressed in equation 16. It is assumed that there is a linear relationship between resistance factors R_u, R_v and R_w, and the velocity vector ν in order to simplify the model.

$$\tau_{res}(\nu) = R\nu = \begin{bmatrix} R_u & 0 & 0 & 0 & 0 & 0 \\ 0 & R_v & 0 & 0 & 0 & 0 \\ 0 & 0 & R_w & 0 & 0 & 0 \\ 0 & 0 & 0 & 0 & 0 & 0 \\ 0 & 0 & 0 & 0 & 0 & 0 \\ 0 & 0 & 0 & 0 & 0 & 0 \end{bmatrix} \tag{16}$$

Inserting equation 13 into equation 8, the kinematics can be expressed as

$$\dot{\nu} = M^{-1}(\tau_{act}(\nu, u) - \tau_g(\eta) - \tau_{res}(\nu) - C(\nu)\nu) \tag{17}$$

2.4 Forces acting on the drone

Multicopter UAV flight is controlled by adjusting the thrust force produced per rotor. The thrust force of a single rotor, here denoted by $F_{Prop,i}$, is a force pointing along the rotational axis of the rotor, and is counteracted by the gravitational force F_G and the drag force F_D. The gravitational force is a downward acting force caused by gravity acting on the drone, pushing the UAV towards the ground. The drag force is a force acting in the opposite direction of the direction of movement of the drone. It is caused by the resistance of the drone colliding with the air, as well as the friction created as the air flows around the drone body. During movements where the UAV is moving at constant speed, these forces are in equilibrium. A multicopter UAV is typically modeled using a 6 degrees of freedom model, where the model allows for three different rotational directions and

3 linear movement directions. The rotational directions are roll ϕ, pitch θ and yaw ψ. This is illustrated below in figure 4.

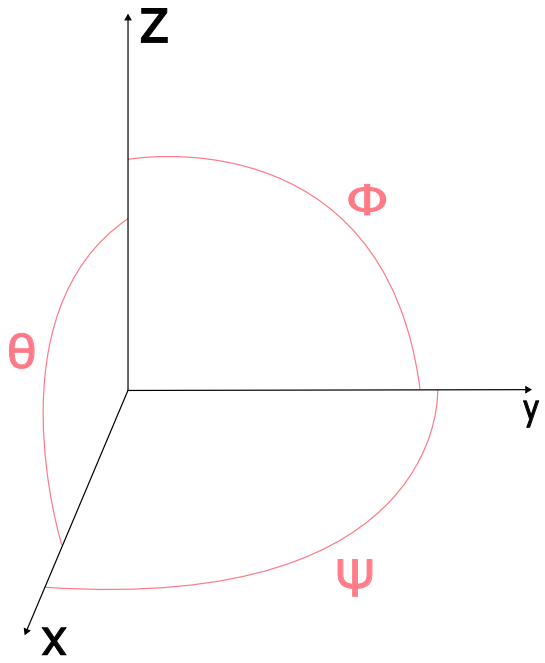

Figure 4: The 6 degrees of freedom illustrated.

In order to maneuver a multicopter, varying amounts of force must be exerted by each rotor. For example, forward flight is achieved by having the rear rtotrs produce increased force compared to the front rotors. Illustrations of the forces are provided later in the chapter.

2.4.1 Drag forces

The drag force affecting the drone can be described as a combination of three drag forces called Profile drag, Induced drag and parasitic drag. The general drag equation is given as $D = \frac{1}{2}A\rho C_d A v^2$.

Induced drag is a type of drag that is a result of creating lift. The induced drag is a component of the total force created by the blades of the UAV rotors, as shown in figure 5 [38].

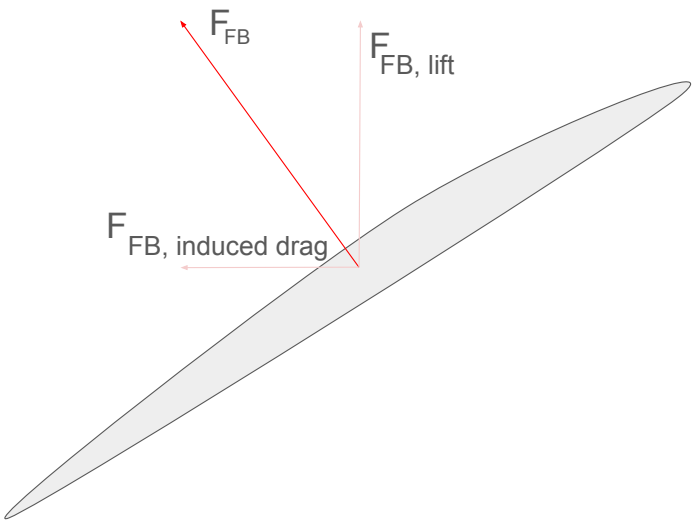

Figure 5: Illustration of the cross section of a single fan blade showing the components of the force exerted by the fan blade. The forces shown in the figure are the force generated by the moving fan blade F_{FB} and its components $F_{FB,induceddrag}$ and $F_{FB,lift}$.

Parasitic drag is the resistance stemming from the friction between the air and the non-rotor parts of the UAV. It depends on the shape of the UAV and increases exponentially with its travel speed as shown by equation 18.

$$F_{Par} = \frac{1}{2}\rho C_D A v^2 \tag{18}$$

Profile drag is a type of drag that affects the fan blades as the rotors spin to generate lift. It acts around the rotor axis in the opposite direction of the rotation, and can be viewed as a parasite drag force that is specific to the rotors of the copter. Due to being a direct resistance to the rotation of the propellers, this is a force that increases with propeller rotation speed. As the propeller rotation speed is instrumental in controlling the movements of the UAV, profile drag is a major factor in determining the amount of power used by the drone.

2.5 Movements

During a real world scenario, a multicopter UAV is able to perform a multitude of both simple and complex movements, many of which woukd require incredibly complex calculations in order to simulate. Therefore, in order to be able to perform simulation and calculation for the movements of the UAV, only simple linear movements will be considered.

2.5.1 Hovering

Hovering is defined as "remaining in place in the air"[37], meaning the drones' position is stationary and has a vertical distance relative to the ground that is non-zero. During hover the only forces

acting on the drone are gravity and the propeller force, which in this case is equal to the lifting force from the rotors of the UAV. In order to achieve stationary hovering, the lifting force must be of equal magnitude to the gravitational force, according to newtons first law [36]. The equilibrium is illustrated in figure 6. In order to more easily illustrate the equilibrium state, the propeller forces are combined into a single force acting on the CG of the UAV.

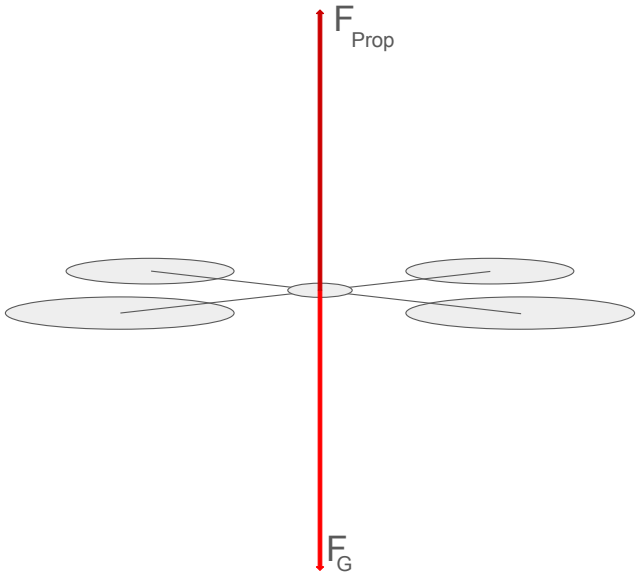

Figure 6: A sketch showing the forces acting on a quadcopter during hover. The propeller forces are illustrated as a single force along the z-axis in order to simplify the illustration.

The equilibrium can also be expressed mathematically as shown in equation 21.

$$\Sigma F = 0 \tag{19}$$

$$\Sigma F = F_L + F_G = ma = 0 \tag{20}$$

$$F_L = ma - F_G = ma + mg = mg \tag{21}$$

2.5.2 Vertical movement

During vertical movement, the forces on the drone are the propeller force, which is equal to the lifting force, the gravitational force and a drag force point in the opposite direction of travel. This is shown in figures 7 and 8, which show forces during ascent and descent respectively.

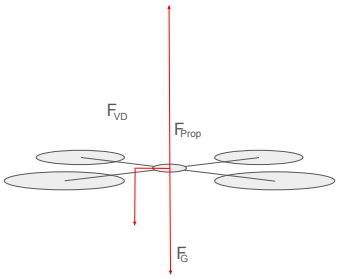

Figure 7: Forces during ascent

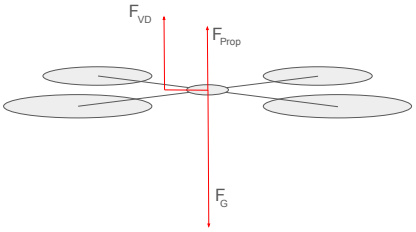

Figure 8: Forces during descent

The equilibrium in these scenarios are described by equations 22 and 23, but an intuitive understanding can be more easily gained from the simplified equations 24 and 25. For sufficiently slow vertical movement, the drag parasitic drag acting on the drone can be considered to be approximately zero.

$$Ascent : F_L = F_G + F_D \tag{22}$$

$$Descent : F_L = F_G - F_D \tag{23}$$

$$Ascent : F_L > F_g \tag{24}$$

$$Descent : F_L < F_g \tag{25}$$

2.5.3 Horizontal movement

the horizontal movement is determined by three forces: propeller force, gravity and air resistance. In this scenario, the propeller force can be decomposed into a vertical and a horizontal component, which will be referred to as lift force and push force respectively. For constant velocity forward flight, the drone is in an equilibrium state where drag force, push force, lift force and gravitational force, denoted by F_D, F_P, F_L and F_G respectively, produce a net zero sum of forces on the drone.

Assuming the forces from the propellers are evenly distributed among them, the magnitude of the lift force per propeller is determined by equation 27.

$$F_G = n \cdot cos(\theta) F_i \tag{26}$$

$$F_i = \frac{F_G}{n \cdot cos(\theta)} \tag{27}$$

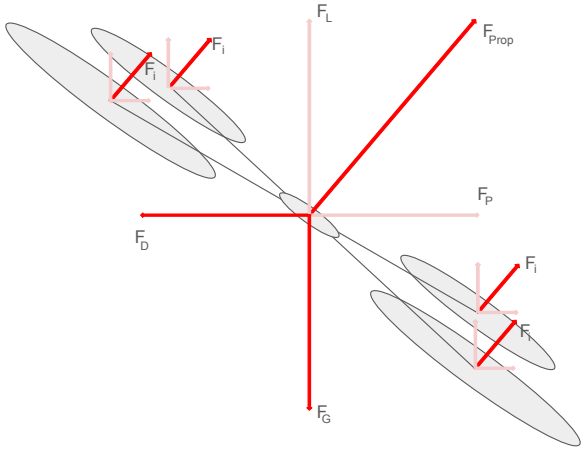

Figure 9: Illustration of a quadcopter UAV showing forces acting upon it, as well as components of decomposed forces being shown in lighter colours.

$$F_D = F_{Prop} \cdot Sin(\theta) \tag{28}$$

$$F_G = F_{Prop} \cdot Cos(\theta) \tag{29}$$

The Pitch angle for a given horizontal speed can be found by using equation 30 [10].

$$mg \cdot tan(\theta) - \frac{1}{2}\rho A C_D v^2 = 0 \tag{30}$$

2.6 Control allocation

There are multiple configurations that can be used for a multicopter, with options having different numbers of rotors, and both flat and coaxial configurations. While UAVs exist that use a coaxial propeller configuration, only flat configuration will be considered in this thesis. This is done both in order to reduce the complexity of the calculations in the thesis and model, and because a loss of efficiency has been observed in the case of coaxial rotors [14].

In order to be able to fly the UAV, it is beneficial to perform control allocation [40]. Control allocation is used to reduce the amount of inputs required to control a system, and to properly divide the forces exerted by the system across the actuators of the system. The concept has is origins in standard state-space form, where $\dot{x} = Ax + Bu$. It is based around finding a unique vector u which satisfies all solutions of equation 31, where ν, B and u represent the forces, the control allocation matrix and the inputs respectively. [40]

$$\nu = Bu \tag{31}$$

$$= \begin{bmatrix} F_x \\ F_y \\ F_x \\ \tau_x \\ \tau_y \\ \tau_z \end{bmatrix} \Rightarrow B \begin{bmatrix} f_{p,1} \\ f_{p,2} \\ f_{p,3} \\ f_{p,4} \end{bmatrix} \tag{32}$$

In this thesis, the control allocation used by Årsandøy will be utilized. The control allocation utilized groups the forces and torques into heave, roll and yaw, which are expressed through the individual force generated by each rotor along the rotor axis [10], and is expressed on a per rotor basis as

$$\begin{bmatrix} F_z \\ \tau_x \\ \tau_y \end{bmatrix} = \begin{bmatrix} 1 \\ -l_2 \\ l_1 \end{bmatrix} f_3 \tag{33}$$

where

- F_z is the force produced by the rotor along the rotor axis, expressed through f_3
- τ_x and τ_y are the torques around the x and y axes respectively
- f_3 is the force produced by the rotor along the rotor axis, presented as a variable
- l_1 is the distance from the CO to the hub of a rotor along the x-axis of the body frame
- l_2 is the distance from the CO to the hub of a rotor along the y-axis of the body frame

In order to ensure proper mapping and distribution to the quadcopter actuator, a standardized control matrix is developed. In Årsandøy's paper, yaw is incorporated in addition to the aforementioned forces and torques, and is expressed as alternating positive and negative ones(1) according to the right hand rule. The final allocation matrix is thus expressed as shown in equation 34

$$\begin{bmatrix} F_z \\ \tau_x \\ \tau_y \\ \tau_z \end{bmatrix} = \begin{bmatrix} 1/n & 1/n & 1/n & 1/n \\ -l_{2,p1} & -l_{2,p2} & -l_{2,p3} & -l_{2,p4} \\ l_{1,p1} & l_{1,p2} & l_{1,p3} & l_{1,p4} \\ 1 & -1 & 1 & -1 \end{bmatrix} \begin{bmatrix} f_{3,p1} \\ f_{3,p2} \\ f_{3,p3} \\ f_{3,p4} \end{bmatrix} \tag{34}$$

In this equation, n is the total number of rotors and p_i denotes the rotor in question.

3 Power consumption

A quadcopter in flight with a constant speed is in an quilibrium as shown in chapter 2. As stated in [30], the overwhelming majority of power being consumed by a quadrotor is used to overcome the drag forces affecting it. These drag forces produce what is known as power losses, which is the power required to overcome them. The total total power losses can be expessed as a sum of the individual drag power losses, as shown in equation 35.

$$P_{tot} = P_i + P_{Par} + P_p \tag{35}$$

where

- P_i is the power loss caused by induced drag
- P_{Par} is the power loss caused by parasitic drag
- P_p is the power loss caused by profile drag

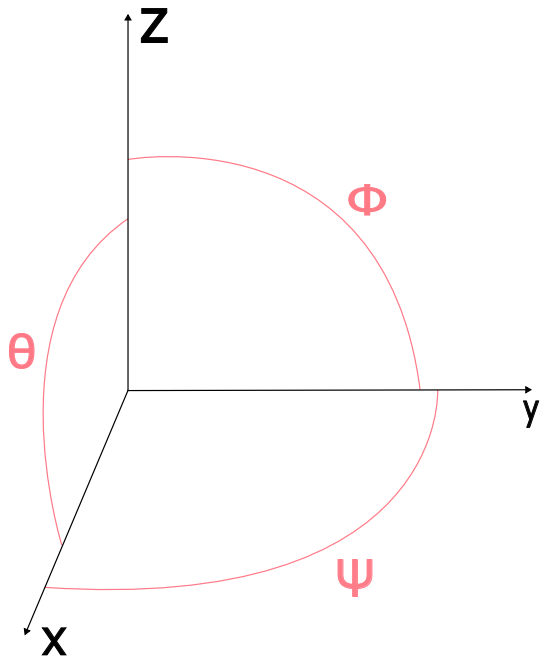

Figure 10: The 6 degrees of freedom illustrated.

3.0.1 Induced losses

the induced losses are defined somewhat differently depending on the source used. In [30], the following model is developed.

$$P_i\left(T, V_{\text{vert}}\right) = k_1 T\left[\frac{V_{\text{vert}}}{2} + \sqrt{\left(\frac{V_{\text{vert}}}{2}\right)^2 + \frac{T}{k_2^2}}\right] \tag{36}$$

Induced losses are the power losses caused by induced drag. The presence of this force is directly caused by the generation of lift, and depends on the velocity of the lift generating bodies and their angle of attack. Induced losses are usually stated to be decreasing with higher velocity. This statement relies on the assumption that the amount of lift generated remains constant[20]. This concept is applied to a wing in an illustration in figure 11.

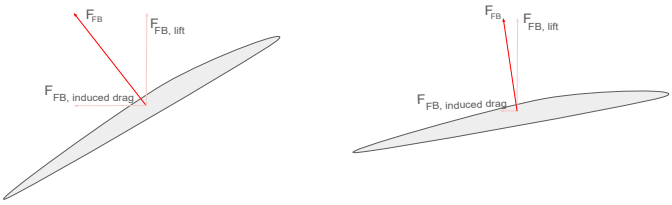

Figure 11: An illustration of the forces produced by a fixed wing at different angles of attack at the speed required to produce said lift.

The induced losses are defined somewhat differently depending on the source used. In [30], the following model is developed.

$$P_i\left(T, V_{\text{vert}}\right) = k_1 T\left[\frac{V_{\text{vert}}}{2} + \sqrt{\left(\frac{V_{\text{vert}}}{2}\right)^2 + \frac{T}{k_2^2}}\right] \tag{37}$$

Matras and Pedersen developed an alternative way of modeling the induced power losses, which was then utilized by Årsandøy in their thesis [10]. This model is based on the linearised Euler equation and Fourier analysis, and accounts for the interference between the airflows of the multiple rotors on a multicopter [10]. The model is stated on a linear time invariant system on a state-space form, where $\nu = [\nu^1\, \nu^2\, \cdots\, \nu^n]^T$ and $\tau = [\tau^1\, \tau^2\, \cdots\, \tau^n]^T$ correspond to inflow and force respectively. The model can thus be stated as

$$\nu = L\tau + \ D\tau \tag{38}$$

$$P_i = T\nu \tag{39}$$

where L and D indicate downward flow underneath the rotors.

3.0.2 Parasitic losses

The parasitic drag force is given by equation 18, as shown in chapter 2, and the relationship between force, speed and power is given by 40.

$$P = Fv \tag{40}$$

Applying the parasitic drag force given by equation 18 in equation 40, an equation can be formulated that gives the parasitic losses as a function of horizontal speed. This relationship is shown in equation 41. It is worth noting that the parasitic drag losses increase proportionally to the cube of the horizontal velocity of the UAV.

$$P_{Par} = \frac{1}{2}\rho C_D A v^3 \tag{41}$$

3.0.3 Profile losses

According to the Embry-Riddle Aeronautical University (AEAU) [23], the profile losses can be expressed as

$$P_p = \frac{1}{8}\rho N \omega^3 c c_d R^4 \tag{42}$$

where

- ρ is the density of air
- N is the number of fan blades on the propeller
- ω is the angular velocity of the fan blade
- c is the blade chord width
- c_d is the drag coefficient of the fan blade
- R is the fan radius

This is further supported by Zhilong et.al. [30]. in their paper, they found that the profile power could be expressed as

$$= \sum_{i=1}^{M} \left(\frac{N c c_d \rho R^4}{8} \left(\Omega_i^3 + \left(V_{air} \cos \alpha_i / R \right)^2 \Omega_i \right) \right) \tag{43}$$

$$= \sum_{i=1}^{M} \left(\frac{N c c_d \rho R^4}{8} \omega_i^3 + \frac{N c c_d \rho R^2}{8} (V_{air} Cos \alpha_i)^2 \omega_i \right) \tag{44}$$

The findings made by Zhilong et.al. align with the model made by AEAU in the case where the the horizontal velocity for the copter is zero, and add an additional term to include situations where forward travel is taking place. It is worth noting that the model found by Zhilong et.al. is stated on a per rotor basis, with the index i denoting the specific rotor. The model is further simplified into the form given in equation 45.

$$P_p\left(T, V_{\text{air}}\right) = c_2 T^{3/2} + c_3 \left(V_{\text{air}} \cos\alpha\right)^2 T^{1/2} \tag{45}$$

$$T = \sqrt{(mg - (c_5(V_a ir cos(\alpha))^2) + c_6 T) + (c_4 V_a ir^2)^2} \tag{46}$$

The last equation lumps all the rotors into one, and assumes the total profile power losses during forward flight will be similar to a case wherein each rotor is modeled separately.

3.0.4 Summary of losses

parameter	analytical expression
k_1	constant $\in [0, 1]$
k_2	$\sqrt{2\rho A}$
c_1	k_1/k_2
c_2	$k_3^{1.5} N c c_d \rho R^4/8$
c_3	$k_3^{0.5} N c c_d \rho R^2/8 \approx 0$
c_4	$C_d \rho A_{quad}/2$
c_5	$\frac{N c c_l \rho R}{A}$
c_6	$\frac{k_3 N c c_l \rho R^3}{6} \approx 0$

Table 1: The table contains the constants used in the model developed by [30]

$$P_i\left(T, V_{\text{vert}}\right) = k_1 T \left[\frac{V_{\text{vert}}}{2} + \sqrt{\left(\frac{V_{\text{vert}}}{2}\right)^2 + \frac{T}{k_2^2}}\right] \tag{47}$$

$$P_p\left(T, V_{\text{air}}\right) = c_2 T^{3/2} + c_3 \left(V_{\text{air}} \cos\alpha\right)^2 T^{1/2} \tag{48}$$

$$P_{\text{par}}\left(V_{\text{air}}\right) = c_4 V_{\text{air}}^3 \tag{49}$$

$$T = \sqrt{\left(mg - \left(c_5 \left(V_{\text{air}} \cos\alpha\right)^2 + c_6 T\right)\right)^2 + \left(c_4 V_{\text{air}}^2\right)^2} \tag{50}$$

3.1 Movements

the movements described in chapter 2 require specific thrust forces, which can be described as a sum of power requirements. These are the power requirements for overcoming the drag forces affecting the UAV during the described movements, and can thus be expressed as a sum of parasitic losses, induced losses and profile losses.

3.1.1 Hovering

During hover, the parasite power of a drone is equal to zero, meaning the power consumption is given as shown in equation 53.

$$P_{hover} = P_p + P_i \tag{51}$$
$$= (c_2 + c_1)T^{\frac{3}{2}} \tag{52}$$
$$= (c_2 + c_1)(mg)^{\frac{3}{2}} \tag{53}$$

3.1.2 Vertical movement

It is assumed that the drone moves slowly enough that parasite drag is not a factor. The resulting expression is given in equation 55.

$$P_{ascent} = P_i + P_p \tag{54}$$
$$= k_1 mg \left[\frac{V_{\text{vert}}}{2} + \sqrt{\left(\frac{V_{\text{vert}}}{2} \right)^2 + \frac{mg}{k_2^2}} \right] + c_2 (mg)^{3/2} \tag{55}$$

3.1.3 Horizontal movement

During forward flight, both Parasite drag, induced drag and profile drag contribute significantly to total power consumption. The total power consumption can therefore be modeled as shown in equation 59.

$$P_{horizontal} = P_i + P_p + P_{par} \tag{56}$$
$$= P_i + P_p + P_{par} \tag{57}$$
$$= k_1 T \sqrt{\frac{T}{k_2^2}} + c_2 T^{3/2} + c_4 V_{\text{air}}^3 \tag{58}$$
$$= (c_1 + c_2)T^{3/2} + c_4 v_{air}^3 \tag{59}$$

4 Laws and regulations

4.1 Classification of UAVs

A UAV is defined as "A powered, aerial vehicle that does not carry a human operator, uses aerodynamic forces to provide vehicle lift, can fly autonomously or be piloted remotely, can be expendable or recoverable, and can carry a lethal or nonlethal payload. Ballistic or semi-ballistic vehicles, cruise missiles, and artillery projectiles are not considered unmanned aerial vehicles" [47], and can be divided into several subclasses. The subclass most relevant to this thesis is copters, a category used for heavier-than-air UAVs using either one or multiple rotors to generate lift. These can be further divided into single rotors, which use only a single lift generating rotor, and multirotors/multicopters, which by definition use two or more, but most commonly use either 4, 6, or 8 lift generating rotors. The focus of this thesis will be quadcopter, which are multicopters using 4 lift generating rotors, as they are the most commonly used [32]. In the rest of the report,the words "drone", "UAV" and "quadcopter" will be used interchangeably, meaning quadcopter.

Most drone operations require categorisation based on some important parameters. These parameters include both drone properties and operation limits. Among these parameters are drone take off mass, distance to building and people, height above ground level (AGL) and requirements of visual line of sight(VLOS) to the drone during operation. There are three operator licenses called RO1, RO2 and RO3 (RO being short for Remotely Piloted Aircraft Systems (RPAS) operator) which can be granted to pilots. These include limitations on what type of aircraft the operator can pilot and the type of operation they are allowed to carry out. It is important to note that the use of "RPAS" instead of "Unmanned Aerial System" (UAS) implies these licenses only allow for operations where the pilot is in constant manual control of the drone [1]. An overview of the three RO license types is given in table 2

	RO 1	RO 2	RO 3
AGL	120 m	120 m	120 m but can also be more*
Safety distance to people, motor vehicles or building not under the pilot's and commander's control	50 m	50 m	50 mbutcan also be less*
Safety distances close to population of more than 100 people	150 m	150 m	150 m but can also be less*
MTOM	$2,5$ kg	25 kg	$>$ 25 kg
Maximum speed	60knop $\approx$ 30 m/s	80knop $\approx$ 41 m/s	$>$ 80knop or powered by a turbine engine
Types of operation	VLOS	VLOS, EVLOS and BLOS	VLOS, EVLOS and BLOS
Light	Daylight	Any	Any

Table 2: An overview of the boundaries of RO 1,2 and 3 drone pilots. [10]

Norwegian law classifies drone operations into three categories: open category, specific category and certified category [48]. The category in which one operates is determined by a series

of parameters of the operation and the equipment used. A simplified view of the categories is provided in figure 12.

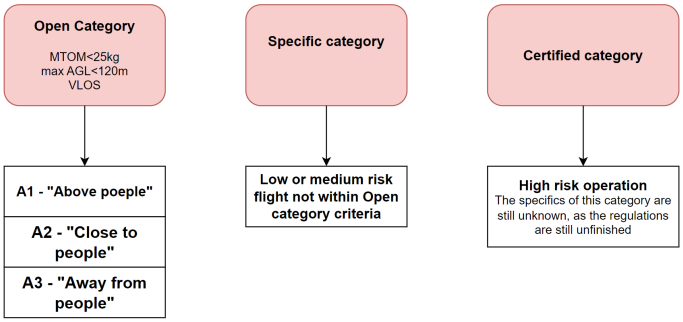

Figure 12: This diagram shows a simplified view of how the flight categories are organised.

4.2 Open category

Operations classified as Open category are limited to using relatively light aircraft, low altitude flight, constant visual line of sight (VLOS) with the UAV and no hazardous cargo, among other requirements. There are some criteria that are enforced across all Open category operations, such as: a maximum MTOM of 25kg, a maximum AGL of 120m, required VLOS,

- Maximum MTOM of 25kg
- Maximum AGL of 120m
- Required VLOS
- No transport of dangerous goods
- Flight above crowds is prohibited

There is also a minimum age limit of 16, where any pre-built drone that is not classified as a toy under C0 classifcation requires the operator to be above this age. As shown in the figure above, the open category is divided into three subcategories called A1, A2 and A3.

4.2.1 A1 - ”Above people”

In this subcategory, an operator below 16 years of age is allowed to fly a self built drone under 250g that flies at speeds under 19m/s. Operators above 16 years of age can fly any drone weighing up to 250g if it was available before January 1st 2024.

4.2.2 A2 - ”Close to people”

An operator flying in this category can use any C2 marked drone. They have to keep at least 30 meters horizontal distance while flying normally, and at least 5 meters when flying in slow mode. In addition to this, the operatpr must follow the 1:1 rule, which states that the drone must have

at least as much distance to people as it has to the ground. All of this can be illustrated as shown in figure 13.

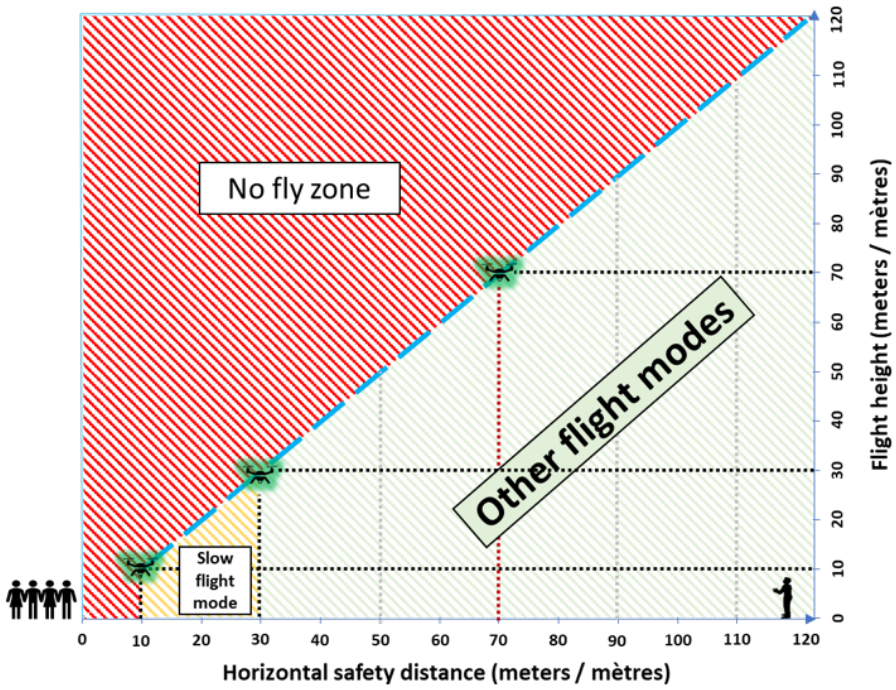

Figure 13: An illustration of the airspace the the operator in an A2 operation is allowed to fly in [39].

4.2.3 A3 - "Away from people"

This subcategory allows for use of C2,C3 and C4 marked drones. Flying in this subcategory, the drone must stay at least 150m from residences, industrial areas and recreational areas. There should be no person present who isnt involved with the operation, and if someone does enter the operation area, the drone is to stay at least 30m from them at all times. The 1:1 rule also applies.

4.3 Specific category

Specific category operations are significantly differentiated from open category by the requirement of confirmation or approval of the operation. This can be done in several different ways, described below and illustrated in figure 14.

4.3.1 Specific Operation Risk Assessment(SORA) / Predefined Risk Assessment(PDRA)

SORA contains information regarding the parameters of the drone that is used, the operation, the risk of someone on the ground getting hit by the UAV, the measures taken to prevent that and the risk of colliding with other aircraft. Each of these contribute to determining the Operational Safety Objectives (OSO), which define the necessary training, safety systems and procedures for the operation. PDRA is a type of predefined SORA that is based on operations given by the

European Union Aviation Safety Agency (EASA), and is divided into 5 operations: PDRA-S01 and -S02, and PDRA-G01, -G02 and -G03 [43]. Using PDRA is meant to be an easier alternative to manually creating a SORA.

1. Create a **ConOps**. ConOps is short for Concept of Operation, and contains information of the most fundamental aspects of the operation. The points that have to be clearly stated in this document are weight and size of the UAV, whether flight is to be done in VLOS or BVLOS, the area underneath the airspace involved in the operation, what airspace is involved in the operation. The weight of the drone is given as MTOM, and the size is the largest characteristic dimension. The size is typically given by wingspan for fixed wing aircraft and diagonal length between rotors on a multirotor.

2. Determine the **Intrinsic Ground Risk Class (GRC)**. GRC is expressed as a number between 1 and 10. This is determined by using a table which contains some properties of the UAV and the ground area that is in proximity to the operation. Using characteristics like UAV size and population size in flight area, as well as expected kinetic energy and line of sight to the drone, a GRC can be found..

3. Determine the **Final GRC**. It is determined by a combination of Intrinsic Ground Risk and measures taken to mitigate the ground risk. These measures are divided into M1, M2 and M3 categories, with M1 being focused around reducing the population put at risk during the mission, M2 being focused on reducing the amount of kinetic enrgy in the event of a collision, and M3 being focused on emergency response in the event of a collision.

4. Determine **Initial Air Risk Class (ARC)**. ARC is determined by operation air space class and flight altitude. It is given as an Airspace Encounter Category (AEC) class from AEC 1 through AEC 12, and and ARC-a, -b, -c or -d.

5. Determine **Residual ARC**. ARC is dependent on initial ARC and strategic measures taken to reduce the air risks. These measures can be things like limiting the operation area, changing the time the operation is carried out or speed up the execution of the operation. It is also possible to perform an analysis of the airspace and improve the risk assessment, assuming the airspace meets the right criteria. Additionally, if the operation is taking place under an altitude of 500m, certain situations can allow for unique adaptation of the rules.

6. Ensure **Tactical Mitigation Performance Requirements (TMPR)** are met. TMPR are a set of five points that must be addressed for a given operation: Detect, decide, command, execute and feedback loop. These points govern how the UAV and operator handle other aircraft in the operation airspace. They contain requirements for detection rates and equipment, how to react upon detection, latency from command to execution, evasion maneuvers to employ and suggestions for drone specs required to perform them, and lastly, update time and latency for intruder position data to reach the operator.

7. Determine **Specific Assurance and Integrity Level (SAIL)**. SAIL is determined based on ARC and GRC. If GRC is determined to be higher than 7, the operation can no longer be classified as Specific category, but is rather a Certified category operation. In order to operate in Specific category, it may be necessary to reevaluate the SORA that was developed.

8. Identify **Operational Safety Objectives (OSO)**. OSO is divided into four levels of importance: Optional, low, medium and high. Depending on the SAIL value determined in the previous step, a set of objectives are determined, each of which is assigned one of the four importance levels. Higher SAIL values mean more objectives will be given higher importance rating.

9. Evaluate risk in nearby airspace in case of loss of control. This step is intended to address what will happen in the event of loss of control or communication, resulting in a fly-away. In order to satisfy this step of the SORA requirements, it must be found through analysis of the UAV that faults with high likelihood of occurrence won't cause a fly-away. In order to avoid this, UAVs often have features that prevent catastrophic failure, such as redundancy or anchor points that the UAV will return to upon loss of communication. Some common examples of faults with high likelihood of occurrence are GPS/GNSS error, compass error, loss of connection, motor fault, or issues with the controller. Each fault included in the evaluation if the system is categorized based on likelihood, ranging from "extremely unlikely" to "happens often". Included with this evaluation of error likelihood is an explanation of the effect it has if it occurs, and countermeasures that can be taken to mitigate the risk or impact. During operation in high traffic airspace, near crowded areas or in restricted areas, it is required that the odds of leaving the operation airspace is less than 1 per 10 000 hours, no single fault can cause the UAV to leave the operation airspace and the UAV must be build to industrial standard.

10. Create a security portfolio containing information on how to reduce risk for GRC and ARC, how to fulfill TMPR, and how to fulfill the OSO requirements. In this portfolio, the previous steps of the SORA are grouped by ConOps, ground risk, air risk, overall risk and documentation. The purpose of the portfolio is to ensure clear communication of how the operator intends to meet operation criteria and mitigate risks.

4.3.2 Standard scenario (STS)

Beginning in 2024, it is possible to declare to operate using a standard scenario. In order to be eligible for this, the drone must meet certain specifications, an Operations manual must be developed, and the operator must pass an exam to get an STS certificate. There may be some overlap between STS and PDRA depending on the governing bodies in the location of the operation, in which case STS is considered easier to use. If an STS matching the desired operation isn't defined in the are one wishes to operate in, using PDRA is necessary. [44] [45]

4.3.3 Light UAS Operator Certificate (LUC)

For large operators, a LUC can be issued which enables them to approve some of their own operations. This is considered a fairly extensive privilege. Therefore, the acquisition process for this certificate is more elaborate than that of a SORA application.[44]

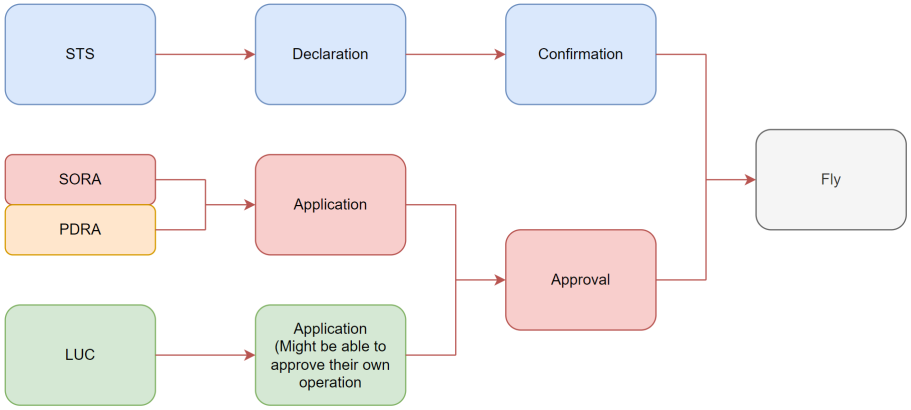

Figure 14: A flow chart illustrating the application process for drone flight approval in Norway.

4.4 Certified category

The third category is the Certified category. The regulations from EASA regarding this category are still unfinished, but is expected to govern high risk flight operations. Examples include flying above large crowds using a drone spanning more than 3m in any direction, transporting people or transporting dangerous goods. Because of the high risk of these operations, they are outside the scope of the other two categories. Until the implementation of the new EASA regulation is done, an approved RO3-application is required.

5 Optimization problem

- the background for why we want to optimize power usage - operation using copter style uavs requires constant power in order to produce lift - therefore, optimizing power consumption is directly connected to extending flight time and/or distance - battery capacity and power usage are integral - the power consumption is caused by the drag forces and lift generation, which is expressed through the drag losses on the body and propellers

The most utilized type of UAV for transportation of commercial goods are multicopters, likely owing to their availability, and balance between maneuverability and speed. These are HTA aircraft, and as such, require constant generation of lift in order to stay airborne. The optimization of power consumption and battery capacity is therefore directly analogous to improving the performance of the UAV, as it can lead to improved endurance, speed or flight distance. The power consumption of a multicopter is directly tied to the mass of the UAV, as well as the mass of any payload it's carrying. While he model developed by Matras and Pedersen that was used by Årsandøy employed a new method for power calculations, it does not include a connection between power consumption and mass.

The relationship between power consumption and mass is important to consider because the increase of mass leads to a necessity for increased lift generation. Considering the complex relationship between the different power losses and lift generation, as well as the effect added mass might have on the horizontal speed capabilities of a multicopter, it is vital to include mass in the model one decides to use.

In the thesis written by Årsandøy, there is emphasis put on finding an optimal speed for a UAV to travel at. This approach is not directly applicable to mass, as any mass increase is guaranteed to increase the overall power requirements for flight. Therefore it is important to examine the relationship between mass and power losses, to acquire an understanding of how quickly the power consumption increases depending on mass.

In order to examine the effect of mass on the power consumption, a similar approach will be taken, where optimums will be found for power related to velocity and distance. While the general approach is similar, a different model for power losses will be employed. The development of the total power will then be examined as more mass is added.

5.1 Objective and constraints

The objective of the optimization problem depends on what is prioritized for a particular use case. In general, the optimization objective is given on the form $minf(x)$ and is typically limited by linear and/or nonlinear constraints. The constraints of this thesis stem partially from the kinetic model of the UAV, and partially from the specifications of each UAV, which often state a maximum travel speed in horizontal and/or vertical directions.

The specific optimization objective used in the use cases discussed in this thesis is the same as one used by Årsandøy, however the main focus is not on the optimization problem itself. The objective is merely to utilize the results of the problem to study the impact of mass, both to see

CPU	Intel I5-9600K
GPU	Nvidia RTX3070
RAM	16GB 3000MHz DDR4
Motherboard	ASUS ROG MAXIMUS XI FORMULA
Storage	Kingston A2000 500GB NVMe M.2 SSD
PSU	EVGA GQ 650W Hybrid Modular 80+ PSU

Table 3: Specifications of the computer used for calculations

if the optimal values change with increased mass, and to observe how quickly the optimum s in relation to a mass increase. That being said, the optimization objectives used were as follows:

Optimal flight range Optimal flight range is achieved through optimizing power per unit of speed $\frac{P}{v}$. This is confirmed through dimension analysis based on the equation $E = Pt$:

$$[J] = [W \cdot s] \tag{60}$$

$$[\frac{J}{m}] = [\frac{W \cdot s}{m}] = [\frac{W}{m/s}] \tag{61}$$

Physics constraints

The constraints of the problem are partly defined based on the kinetics of the quadcopter. During flight, the movements of the drone are simplified to constant velocity, steady state flight paths where all forces and torques are in equilibrium. This is expressed through equation 62, which is utilized as a constraint for the optimization problem.

$$\dot{\nu} = M^{-1}(\tau(\nu) - C(\nu)\nu) = 0 \tag{62}$$

5.2 Implementation

set up the constraints for the operations type

import parameters for each drone

The optimization problem was implemented on a desktop computer running Windows 10. The specifications of the computer are listed below in table 3.

The MATLAB script was written on a form which allows for easy import of parameters from different UAVs. It is worth noting that the model is specific to quadcopter UAV. It was written in MATLAB due to having some previous experience with the software. It was also used because it allows for relatively easy definitions of functions. The software has built in functionality for solving optimization problems, and has excellent documentation. The optimisation problems defined in chapter 5.1 using the *fmincon* function. this function solves problems on the form shown in equation 63.

$$\min_x f(x) \text{ such that } \begin{cases} c(x) \leq 0 \\ ceq(x) = 0 \\ A \cdot x \leq b \\ Aeq \cdot x = beq \\ lb \leq x \leq ub, \end{cases} \tag{63}$$

6 Case studies

In order to perform optimization for a UAV, it is crucial to examine the operating scenario it will be performing in. The use cases for drone technology are varied, and include scenarios like:

- infrastructure inspection
- monitoring and surveillance
- mapping
- transportation

Given that the focus of this thesis is based around drone use in delivery services, transportation will be the main focus when developing case studies. It is worth noting that even within this category, the challenges and priorities of the operation are varied, depending on where it takes place and what is being transported. Therefore, the objective of the case studies discussed in this thesis will be to examine the regulatory requirements for the different operations, to evaluate what aspect of the drone performance is prioritize, and by extension, what the optimization objective for each scenario should be. The scenarios that will be considered in these case studies are:

- Delivery in urban areas
- Delivery in rural and remote areas
- Delivery of medical supplies or equipment

6.1 Case study: Delivery operations in urban areas

Drones have long been used in military application as decoys, for surveillance and reconnaissance, and for offense [49]. It was only in 2013 that drones entered the mainstream, when Jeff Bezos announced amazons intent to perform last mile delivery. Since then, more actors have entered the market, such as Matternet, UPS, Wing and Flytrex [25]. In order for services like this to be viable, they need to be able to operate in a multitude of settings, ranging from remote to urban.

When operating in urban areas, there are multiple challenges to overcome, a lot of which stem from the inherently high risk of operating in highly populated areas. The risk is caused by factors explained in chapter 4. These will have to be accounted for in the SORA for the operation. In order to mitigate the risks of such an operation, it might be possible to choose a flight path and altitude that minimizes risk of hitting bystanders in the event of a fly-away. This might be achievable by flying above the roofs of the area. This would mean that the risk of personal injury is reduced. Additionally, it might be possible to mitigate risk of damage by using smaller drones with less mass. It should be noted that this might also mean reduced carrying capacity per drone. Taking these factors into account, the Aurelia X4 Standard was chosen for this case study, as it's not too heavy, and has a decent ratio of max payload weight to drone mass [12]. It is also hypothesized that a smaller UAV is sufficient to carry most packages in an urban setting, considering the majority of amazons best selling items are fairly light objects (as of 21.01.24) [9].

6.1.1 Drone specifications

In the drone delivery business, it is common for the companies to develop their own aircraft to carry out mission, as indicated by [3]. Because these companies largely use different UAVs, a UAV was chosen that was deemed applicable for this specific use case. The Aurelia X4 was chosen for this case study because it boasts high carrying capacity for its mass, relatively long maximum flight time and low MTOM. Some key specification are provided below in table 4, while the rest can be found on the manufacturer website [11]. Some of the specifications must be calculated based on those stated explicitly, and are marked with a star. The values marked with the star were found using top-down photos and ratios between known measurements to find the unknowns. This was done due to a lack of available information about these measurements online. Before implementation of this model in a real-life scenario, these values should be acquired from the manufacturer or measured manually.

UAV: Aurealia X4 Standard	
Dimensions L × W × H	835 × 835 × 335mm (propellers not included)
Weight	2.450kg (no batteries), 3.924kg (LE batteries included)
MOTM	5.424kg
Max horizontal speed	15.6m/s
Maximum flight time	40 mins

Propeller: Aurelia X4 standard	
Diameter	700mm *
Chord width	50mm *

Battery: Aurelia X4 Long Endurance Li-ion battery	
Weight	1.474kg *
Capacity	16000mAh
Voltage	22.2V

Table 4: SORA for a delivery operation in a city

6.1.2 Flight path / mission scenario

The main advantage of employing a UAV delivery solution in an urban area is the potential for reduced delivery times. This potential stems from multiple factors, the most fundamental of which being that a UAV has the ability to ascend above the roofs of the buildings in the area. This straight flight will in most cases be much faster than delivery by car, as ground traffic can be completely avoided, and straight flight requires few to no turns. In addition to increasing delivery speed, the reduction in delivery vehicles on the roads has potential to alleviate traffic. This solution also has potential to be financially beneficial for delivery companies, as the need for drivers will be eliminated or greatly reduced for last mile delivery. This is predicated on the drones being able to operate autonomously and that the appropriate operation infrastructure is developed.

During an operation of this type, the UAV will likely be required to perform multiple simple and complex maneuvers. In order to perform analysis of the UAV however, the movements considered in this case study will be limited to simple movements as shown in figure 15:

- Ascent: The UAV will be made to ascend to a proper altitude, where the risk of collision with buildings is negligible and the UAV is more likely to land on a roof in the event of a

fly-away. The UAV will also have to ascend to the proper altitude after delivery in order to return to base. Assuming a height per floor in a building is 1.9 meters [17], and that the average building has fewer than 30 floors, a flight altitude of 60m should be sufficient for general operation. It is worth noting that there are taller buildings which need to be accounted for, such as the Radisson Blu Plaza hotel [29].

- Forward flight: After reaching the desired altitude, the UAV will move in a straight line towards the delivery location. After delivery, it will also have to return to base.
- Descent: During delivery, the drone will have to descend to the level of the recipient. It will also have to descend upon returning to base.

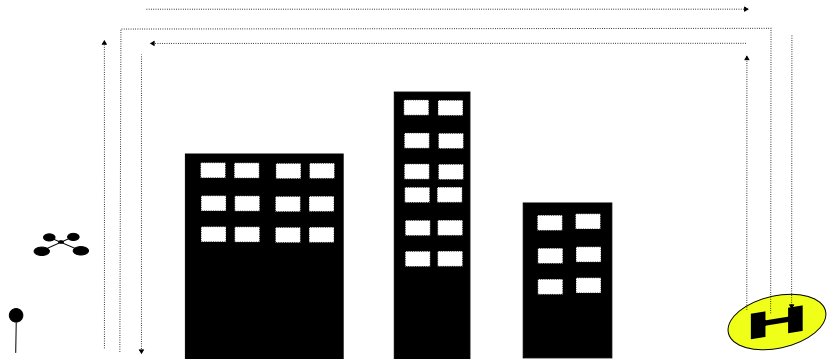

Figure 15: Simplified urban flight path using only linear movements.

6.1.3 Operations category

As this type of operation requires operation outside of VLOS, operating in Open Category is not an option. The operation can be carried out withing the specific category, but requires development of a SORA, as no PDRA is applicable. Developing a SORA for this situation might prove difficult, as flight over a populated area carries inherent risk. It is also possible that defining the flight geography for an entire area of a city might be difficult or impossible. It might be beneficial for the organization doing the delivery to apply for a LUC, in which case they would be able to define a Flight geography per drone flight and, provided the SORA is reasonable, approve their own missions. Regardless of acquisition of a LUC, the SORA for each operation must include documentation regarding the intended operation procedures, the risks, the contingencies and the OSOs for the operation, as stated in chapter 4. Table 5 contains some key values which provide an overview of a SORA for this type of operation.

Operation type	BVLOS
Area	Populated
Height	Maximum 120 m

Inherent ground risk				6
Mitigation	M1 = −1	M2 = 0	M3 = 0	-1
Final ground risk (GRC)				5

Initial air risk	ARC-C
Residual air risk	ARC-B

SAIL	IV

Table 5: SORA for a delivery operation in an urban area.

This is an example of one possible SORA that could be utilized, as there isn't yet a predefined SORA or PDRA for this type of operation. IT would be beneficial to implement safety measures to reduce the risk if possible, as that would allow for lower SAIL-levels and less restrictive operation parameters. It would for example be possible to conduct detailed analysis of population density in an are related to time of day, which could allow for transport to occur mostly during less active hours.

6.2 Case study: Delivery in rural and remote areas

Operation in a remote or sparsely populated area is quite different with regard to regulations than in an urban area. This is in large part due to the lower population density causing a significant reduction in ground risk. The air risk is also reduced. it should be noted that there are still significant advantages to maintaining high altitudes, as there is risk of collision with electrical poles, trees or houses.

When doing delivery in remote areas, the distance from the base station to the delivery point might be considerably larger than in an urban setting. It is therefore important to choose a UAV with good flight range. The carrying capacity of the UAV is also a significant factor in this case, as it might be beneficial to perform fewer flights with more load to far away locations, rather than flying more trips with less load. Because of these considerations, the Keel Quadcopter Deliver Drone was chosen for this case study. It was chose because it is a UAV with long flight time and relatively high payload capacity. An additional benefit of this UAV is that the attachments to the drone are fairly modular, meaning the drone could make multiple deliveries in one trip using multiple payload attachments.

6.2.1 Drone specifications

For this application, long range was prioritized. The Freefly Alta X has a relatively long maximum flight time of 50 minutes [6], as well as a high carrying capacity.

This UAV was chosen due to its relatively good endurance, high carrying capacity and array of customization options. The UAV can be fitted with an array of cameras, sensors

Some key specifications are provided in table 6

UAV: Freefly ALTA X	
Dimensions L × W × H	1000.6 × 1000.6 × 387mm (propellers not included)
Weight	10kg (no batteries)
MOTM	34.86kg
Max horizontal speed	26.38/s
Maximum flight time	50mins

Propeller: 33x9in	
Diameter	840mm
Chord width	102mm *

Battery	
Weight	4.47kg per battery
Capacity	16000mAh
Voltage	44.4V

Table 6: SORA for a delivery operation in remote and sparsely populateed areas

6.2.2 Flight path

The flight path for this mission is likely to involve a combination of vertical, horizontal and diagonal movements, however, in this thesis, only straight flight will be considered. It is important to maintain enough altitude that collision is a non issue. It is also wise to avoid roads and populated area as best as possible to avoid risk of property damage or injury.

6.2.3 Operations type

Much like the previous case study, this operation will largely take place outside of VLOS, which means that this case also isn't suitable for open category operation. within specific category, it can be argued that this operation can be carried out under PDRA-G01[7]. This PDRA allows flight over sparsely populated areas up to 120m AGL, however it also stipulates stat there must be no more than 1 kilometer from the UAV to the closest airspace observer. It also specifically states that no fully autonomous operation can take place in this category, and that and operator must at all times be able to assume manual control of the UAV. It also states that the operator may not operate more than one UAV at a time, limiting the operation to one delivery trip at a time, and eliminating the possibility of using a fleet of drones for delivery. A SORA is outlined in table 7 which might apply to this use case. As in the previous case study, it might be beneficial to acquire a LUC in order to be able to operate consistently.

Operation type	BVLOS
Area	Sparsely populated
Height	Maximum 120 m

Inherent ground risk				4
Mitigation	M1 = −1	M2 = 0	M3 = 0	-1
Final ground risk (GRC)				3

Initial air risk	ARC-B
Residual air risk	ARC-B

SAIL	II

Table 7: SORA for a delivery operation in a city

6.3 Case study: Delivery of medical supplies

When transporting medical supplies, it can be argued that there are a lot of cases where delivery time is crucial, such as in the event of a heart attack where a defibrillator is needed, or if an organ transplant is needed. In both of these cases, optimizing for either flight time or distance is only a secondary objective compared to achieving the fastest possible delivery time. With regards to that, it is essential to know how much a payload is going to affect the range at maximum speeds.

During operations like these, an argument could be made that they often take place as part of the state aviation category, which uses RO2 and RO3 are required [27]. An overview of the RO types is given in chapter 4. It should also be noted that these kinds of operation aren't inherently tied to a specific type of landscape or population density, meaning the exact mission details with regards to ground and air risk would likely vary greatly on a per mission basis. Given the relatively high velocity of the Freefly ALTA X, it was chosen for this mission type as well.

6.3.1 Drone specifications

The Freefly ALTA X was chosen for this operation, as it has relatively high maximum speed, relatively good endurance and good carrying capacity. This means the UAV should be greatly adaptable, and should be suitable for a range of missions. The specifications of the UAV were state previously, although due to the nature of this type of mission and the relatively rare nature of them, it seems likely that an operator will maintain constant control and/or supervision, and a camera will have to be used in order for them to be able to pilot the UAV.

6.3.2 Flight path

The flight path of this case study will be similar to the previous two. In addition to reducing the chance of collision, maintaining a relatively high AGL could provide insight into the geography around the intended drop-off location, and could allow them to assess the severity and urgency of the situation itself.

6.3.3 Operations type

This type of operations is most likely to be carried out by licensed medical personnel, and would therefore be considered state aviation. In order to be able to operate in state aviation missions , RO2 or RO3 certification is necessary. An Overview of the RO-categories is provided in chapter 4, which shows that in order to be able to fly in close proximity to people, RO3 certification is required. RO3 is also a requirement due to the MTOM of the UAV that was chosen.

6.4 Implementation

An overview of the implementation of the case study is provided below. This is a general implementation, not specific to any one case study. The optimization problem was The implementation of an optimization problem is of great significance with regard to determining the computational load of a problem. Here, the power consumption model and drone parameters are given in a separate file called "power_consumption_model_test".

```
% Define the optimization problem
options = optimoptions('fmincon', 'Algorithm', 'interior-point');
initial_guess = [0.5]; % Initial guess

lb = [0]; % Lower bounds
ub = [26];    % Upper bounds

% Solve the optimization problem
optimal_values = fmincon(@power_consumption_model_test,
    initial_guess, [], [], [], [], lb, ub, [], options);

% Extract the optimal values
opt_vair = optimal_values(1);

% Display the results
fprintf('Optimal vair: %.4f\n', opt_vair);
```

7 Model validation

Before implementation of the model in a real life scenario, it must be validated to ensure accurate behaviour. Any assumptions being made in development of the model need to be specified in order to best understand the shortcomings of the model. It is also vital to have a comprehensive understanding of the model in order to be able to troubleshoot, should the results deviate significantly from the expected values. An integral part of the model is the parameters of the UAV that is to be used. These can often be found on the manufacturer website in the data sheet for the drone, or can sometimes be provided upon request from the manufacturer. If these options aren't available for a given drone, the parameters can be found experimentally in a wind tunnel or lab.

7.1 Model validation

In order to validate the model, the UAV calculator eCalc was utilized[50]. It was used by Årsandøy[10] to some success, although she noted that there were some discrepancies between the website and her findings. The calculator was used with the Aurelia X4 UAV. The parameters were input, and resulted in the graph shown in figure 16.

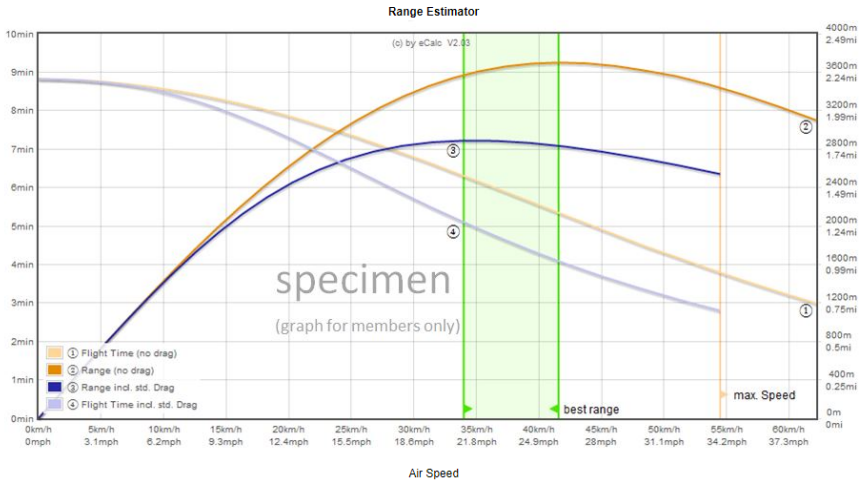

Figure 16: eCalc calculations of various properties of the Aurelia X4's performance.

The graph shows a "best range" of speeds up to 40km/h, or 11.1111m/s when flying the UAV without payload. This is within 10% margin of the 12.2124m/s found in this thesis. These values are considered relatively similar, and are interpreted as reinforcing to the model developed in this thesis, although the difference is worth keeping in mind.

8 Results

In the case studies performed in this thesis, both power and energy consumption were examined in relation to UAV/payload mass in order to establish a relationship between them. The goal was to develop and test a model which improved upon the one used by Årsandøy by including a mass component.

8.1 Urban delivery

For the first case study, the objective was to implement a model which could serve to give an optimal range for a UAV delivery mission, as well as give an accurate image of the power consumption of the UAV. It was implemented in MATLAB using the $fmincon()$ function, and both range and power graphs were plotted, only considering the UAV mass without load in order to confirm that the model aligned with what was expected. The graphs are given below, in figures 17 and 18.

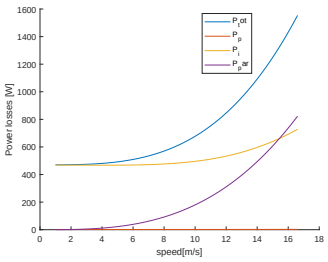

Figure 17: The power consumption and the individual drag losses contributing to it.

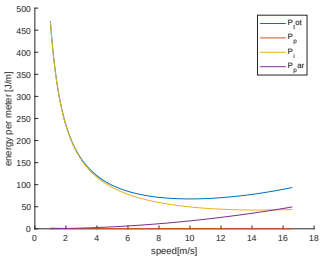

Figure 18: The energy consumption illustrating the optimal speed for maximum range.

The graphs show increasing power consumption with increasing mass, as expected. The range graph also shows the characteristic shape found to be generally applicable to UAV energy optimums, which indicates that the model is realistic.

8.2 Remote delivery

For the second case study, the flight distance was deemed an essential property, and was therefore the objective of study. The problem was implemented in MATLAB using the $fmincon()$ function, with constraints based on quadcopter kinetics. Constraints were also implemented that constrained the minimum and maximum horizontal speeds for the UAV. When implemented in the way that was described, the script returned an optimal value for horizontal speed in order to achieve optimal energy use per meter traveled. The direct outcome of this is that the flight range of the UAV is found to be optimal at this velocity..

This was originally done using only the UAV mass with batteries included, but no payload, in order to confirm that the script was functioning correctly. The payload mass was implemented as an easily changed parameter, meaning it was possible to further utilize the script with changed values. The payload mass was then increased incrementally, and the optimal velocity was examined for each iteration. This is shown in figures 19-24. This was done to examine the change in optimal velocity as mass was increased

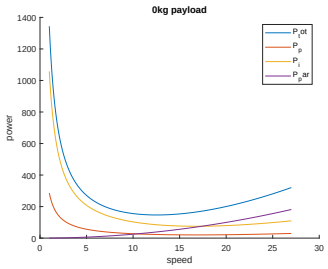

Figure 19: The power consumption and the individual drag losses contributing to it.

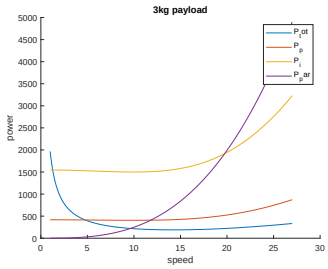

Figure 20: The energy consumption illustrating the optimal speed for maximum range.

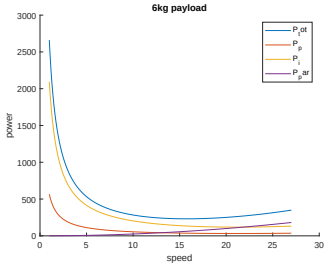

Figure 21: The power consumption and the individual drag losses contributing to it.

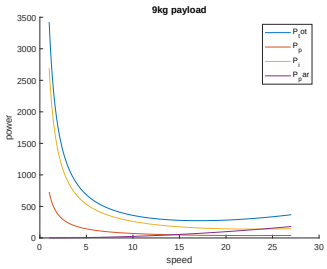

Figure 22: The energy consumption illustrating the optimal speed for maximum range.

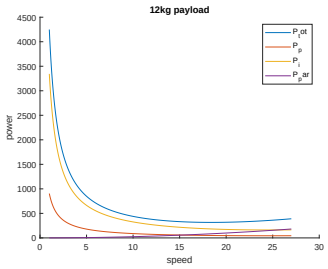

Figure 23: The power consumption and the individual drag losses contributing to it.

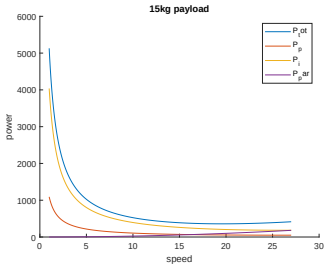

Figure 24: The energy consumption illustrating the optimal speed for maximum range.

These simulations indicate that the optimal speed is increasing with increasing mass, as the

$fmincon()$ functions yielded optimal speeds of 12.2124, 13.8624, 15.3359, 16.6796, 17.9230 and 19.0855 corresponding to payload weights of 0kg, 3kg, 6kg, 9kg, 12kg and 15kg respectively.

8.3 Emergency delivery

In the case of emergency delivery, it was assumed that the most important parameter of the mission was UAV top speed. It was therefore assumed that the UAV would travel at maximum speed for the whole mission. No constraints were implemented based on regulation, as the UAV maximum velocity is considerably lower than the maximum speed of 41m/s[10]. The function that was implemented previously was a function describing range as a function of horizontal speed. In this case study, the range was implemented purely as a function of mass with speed remaining constant. The results are shown in figure 25.

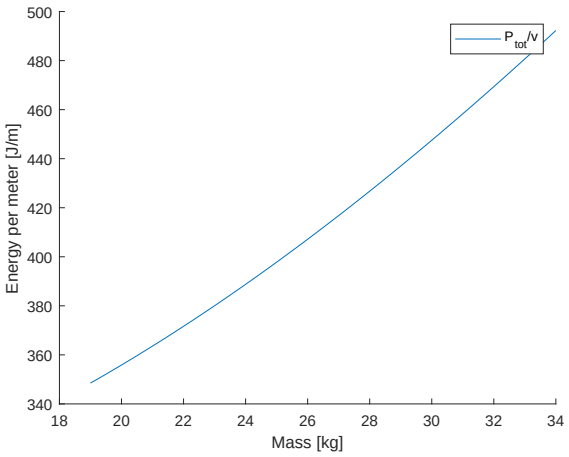

Figure 25: The increase in energy requirements with increased mass.

The graph shows a near linear increase of energy requirements per meter when the mass is increased. It should however be noted that the increase is in fact not entirely linear, and seems to trend towards an exponential increase with higher mass added. This does not seem to be significantly impactful within the carrying capabilities of this particular UAV, and will therefore be deemed beyond the scope of this thesis.

Because the increase found in the case study was found to be nearly linear, it is possible that the mass of the UAV and payload could be simplified to a scaling factor while maintaining relatively good model accuracy. This seems to be entirely predicated on how large of a mass interval is considered. Should this be possible, it would be highly beneficial, as it could significantly reduce the complexity of the calculations needed for accurate simulation.

9 Conclusion

In this thesis, a model has been developed which build on the previous efforts of Årsandøy[10], Matras[33] and Pedersen[42]. The model aimed to incorporate mass into an existing model, and examine the relationship between power consumption and mass. This was done through case studies, which were identified and described in the thesis. These included calculations and optimization done with the aim of gaining insight into the complex interplay between the individual power losses and total power loss, mass and speed. There was emphasis put on trying to achieve an understanding of these operation types with the goal of being able to implement them in a real life scenario. To that extent, information was included on UAV flight regulations in Norway. The effect of mass on the power and energy usage was examined in multiple ways, including optimization of range, examination of this optimum with changing masses and the effect a mass change can have on the overall range of a UAV given constant velocity. This was done so as to arrive at a model that is as comprehensive as possible, while not being too computationally demanding.

The findings of this thesis indicate that a change in mass on a UAV can change the performance characteristics noticeably, as both optimal speeds and range were significantly affected. These are essential factors in planning flight missions and operations, and are therefore integral to the expansion of UAV transport industry. Also essential to these operations are the regulations for unmanned flight, which in many cases aren't well adapted to allow for commercial delivery operations on a large scale. Overall, the results yielded by the optimization and calculations done in this thesis have yielded reasonable results across different UAV models, and with regards to differing objectives.

9.1 Future work

9.1.1 Better data sheets

In this thesis, the UAV models used were chosen largely without regard to whether there was easily accessible data to be found about them. It is worth noting that UAVs like the Keel Quadcopter Delivery drone, which was originally supposed to be used in one use case, were dismissed as candidates due to confusing or even directly conflicting information regarding their performance [26]. The data found during writing of this thesis was not necessarily easy to locate either, with testing data, performance claims from the manufacturer and specifications divided for some of them, even on the manufacturer website. This was particularly noticeable when using the Freefly ALTA X [5]. In the future it would be beneficial for there to be regulations which govern how this information must be presented, in order to more easily be able to perform predictive calculations ahead of an operation.

9.1.2 More real world testing and data publishing

Another point of struggle was the severe lack of independent scientific testing done on UAVs. While the improvements to the data sheets provided by manufacturers mentioned earlier might help, independent testing of products like these is essential in fairly evaluating what equipment to

use for a given operation. Independent testing may also lead to coverage of properties of a UAV beyond what the manufacturer is willing to share, meaning it would be easier to make informed decisions on how to carry out an operation.

9.1.3 Implementation of the model

In order to further test the model and its viability, it would be beneficial to have it tested more thoroughly. This could be done either through more and different case studies, or through real life implementation and testing. This should be done using UAVs of different size and shape, although with the knowledge that the model is developed mainly for a quadcopter. I believe the goal of such testing should be to uncover the limitations of the model, and if possible, simplify it further.

Bibliography

[1] URL: https://www.norwegiandrones.no/kopi-av-aktuelt (visited on 22nd Jan. 2024).

[2] Hasini Viranga Abeywickrama et al. 'Comprehensive Energy Consumption Model for Unmanned Aerial Vehicles, Based on Empirical Studies of Battery Performance'. In: *IEEE Access* 6 (2018), pp. 58383–58394. DOI: 10.1109/ACCESS.2018.2875040.

[3] Alf Alferez. *Top 10 Commercial Drone Delivery Companies*. URL: https://www.ecommercenext.org/top-10-commercial-drone-delivery-companies/ (visited on 22nd Jan. 2024).

[4] Jackie Alkobi. *The Evolution of Drones: From Military to Hobby Commercial*. URL: https://percepto.co/the-evolution-of-drones-from-military-to-hobby-commercial/ (visited on 22nd Jan. 2024).

[5] *Alta X*. URL: https://freeflysystems.com/alta-x (visited on 22nd Jan. 2024).

[6] *Alta X, world's toughest drone*. URL: https://freefly-prod.s3-us-west-2.amazonaws.com/support/alta-x-brochure-v2.pdf (visited on 22nd Jan. 2024).

[7] *Alta X, world's toughest drone*. URL: https://luftfartstilsynet.no/globalassets/dokumenter/dronedokumenter/nytt-eu-regelverk/pdra/pdra-g01-samsvarsmatrise.docx (visited on 22nd Jan. 2024).

[8] Shaikh Altamash, Syed Adnan and Padwekar Aamir. 'KINEMATIC, DYNAMIC MODELING AND SIMULATION OF QUADCOPTER'. In: (2016), p. 16.

[9] *Amazon Best Sellers*. URL: https://www.amazon.com/Best-Sellers/zgbs (visited on 22nd Jan. 2024).

[10] Frida Xiang Nordås Årsandøy. 'Power optimisation of autonomous rotorcraft'. In: (2023).

[11] *Aurelia X4 Standard*. URL: https://aurelia-aerospace.com/product/aurelia-x4-standard/ (visited on 22nd Jan. 2024).

[12] *Aurelia X4 Standard - Ready To Fly*. URL: https://uavsystemsinternational.com/products/aurelia-x4-standard (visited on 22nd Jan. 2024).

[13] Ahmed Bahabry et al. 'Low-Altitude Navigation for Multi-Rotor Drones in Urban Areas'. In: *IEEE Access* 7 (2019), pp. 87716–87731. DOI: 10.1109/ACCESS.2019.2925531.

[14] Adam Bondyra et al. 'Performance of Coaxial Propulsion in Design of Multi-rotor UAVs'. In: vol. 440. Mar. 2016, pp. 523–531. ISBN: Print ISBN: 978-3-319-29356-1, Online ISBN: 978-3-319-29357-8. DOI: 10.1007/978-3-319-29357-8_46.

[15] The editors of encyclopedia britannica. *kinematics*. URL: https://www.britannica.com/science/kinematics (visited on 22nd Jan. 2024).

[16] The editors of encyclopedia britannica. *Power*. URL: https://www.britannica.com/science/power-physics (visited on 22nd Jan. 2024).

[17] *Bruksareal: En komplett guide (definisjon, utregning, krav)*. URL: https://www.meglersmart.no/guide/bruksareal (visited on 22nd Jan. 2024).

[18] *Creatively commercial uses of drones*. URL: https://weareama.com/creatively-commercial-uses-drones/ (visited on 22nd Jan. 2024).

[19] *Drag*. URL: https://skybrary.aero/articles/drag (visited on 22nd Jan. 2024).

[20] *Drag*. URL: https://wiki.ivao.aero/en/home/training/documentation/Drag (visited on 22nd Jan. 2024).

[21] Thor I. Fossen. *HANDBOOK OF MARINE CRAFT HYDRODYNAMICS AND MOTION CONTROL*. John Wiley and Sons, Ltd, 2011. ISBN: 978-1-119-99149-6.

[22] Manuel Ramos Jr. Gene Patrick Rible, Nicolette Ann Arriola. 'Modeling and Implementation of Quadcopter Autonomous Flight Based on Alternative Methods to Determine Propeller Parameters'. In: *Advances in Science, Technology and Engineering Systems Journal* 5.5 (2020), pp. 727–741. DOI: 10.25046/aj050589.

[23] *HELICOPTERS VERTICAL FLIGHT*. URL: https://eaglepubs.erau.edu/introductiontoaerospaceflightvehicles/chapter/helicopters-vtol/ (visited on 22nd Jan. 2024).

[24] Pilot Institute. *Induced Drag Explained*. URL: https://pilotinstitute.com/induced-drag-explained/ (visited on 22nd Jan. 2024).

[25] Dawn Kawamoto. *12 Drone Delivery Companies to Know*. URL: https://builtin.com/drones/drone-delivery-companies (visited on 18th Jan. 2024).

[26] *Keel Quadcopter Delivery Drone*. URL: https://www.worldronemarket.com/product/keel-quadcopter/ (visited on 22nd Jan. 2024).

[27] *Krav for statsluftfart (RO2 og RO3)*. URL: https://luftfartstilsynet.no/droner/veiledning/statsluftfart/krav-for-ro2-og-ro3/ (visited on 22nd Jan. 2024).

[28] Joakim brobakk Lehn. 'Model, Design and Control of a Quadcopter'. In: (2015).

[29] *List of tallest buildings in Norway*. URL: https://en.wikipedia.org/wiki/List_of_tallest_buildings_in_Norway (visited on 22nd Jan. 2024).

[30] Zhilong Liu, Raja Sengupta and Alex Kurzhanskiy. 'A power consumption model for multi-rotor small unmanned aircraft systems'. In: *2017 International Conference on Unmanned Aircraft Systems (ICUAS)*. 2017, pp. 310–315. DOI: 10.1109/ICUAS.2017.7991310.

[31] Harsh Malapur et al. 'Diffused casing of drone propeller for reduced operational noise and optimized energy consumption'. In: *Materials Today: Proceedings* 63 (2022). 4th International Conference on Advances in Mechanical Engineering and Nanotechnology, pp. 136–140. ISSN: 2214-7853. DOI: https://doi.org/10.1016/j.matpr.2022.02.413. URL: https://www.sciencedirect.com/science/article/pii/S2214785322011038.

[32] *Market Report Description*. URL: https://www.kbvresearch.com/multirotor-drone-market/ (visited on 22nd Jan. 2024).

[33] Finn Matras. 'Multiaspect power optimization based on induced flow considerations'. In: (2020).

[34] Viacheslav Moskalenko et al. 'The Model and Training Algorithm of Compact Drone Autonomous Visual Navigation System'. In: *Data* 4.1 (2019). ISSN: 2306-5729. URL: https://www.mdpi.com/2306-5729/4/1/4.

[35] Tarek M. Mostafa, Aam Muharam and Reiji Hattori. 'Wireless battery charging system for drones via capacitive power transfer'. In: *2017 IEEE PELS Workshop on Emerging Technologies: Wireless Power Transfer (WoW)*. 2017, pp. 1–6. DOI: 10.1109/WoW.2017.7959357.

[36] Nasa official Nancy Hall. *Newton's Laws of Motion*. URL: https://www1.grc.nasa.gov/beginners-guide-to-aeronautics/newtons-laws-of-motion/ (visited on 31st Oct. 2023).

[37] Department of Marine Technology NTNU. *Cambridge Dictionary - Hover*. URL: https://dictionary.cambridge.org/dictionary/english/hover (visited on 31st Oct. 2023).

[38] Sammy Omari et al. 'Nonlinear control of VTOL UAVs incorporating flapping dynamics'. In: Nov. 2013. DOI: 10.1109/IROS.2013.6696696.

[39] *Open Category*. URL: https://dac.gouvernement.lu/en/drones/drones-let-me-fly/categorie-open.html (visited on 22nd Jan. 2024).

[40] Jeb Orr. *Control Allocation*. URL: https://nescacademy.nasa.gov/video/5f8436500f7347e6b433eca70e34ed171d (visited on 22nd Jan. 2024).

[41] *Parasite Drag*. URL: https://skybrary.aero/articles/parasite-drag (visited on 22nd Jan. 2024).

[42] Morten Dinhoff Pedersen and Finn Matras. 'Multirotor inflow dynamics'. In: *AmericanInstitute of Aeronautics and Astronautics (AIAA) Journal* (2023).

[43] *Slik søker du om tillatelse for å fly etter en PDRA*. URL: https://luftfartstilsynet.no/droner/registrering-og-soknader/soke-om-tillatelse-i-spesifikk-kategori/soke-om-tillatelse-til-pdra/ (visited on 22nd Jan. 2024).

[44] *Spesifikk kategori*. URL: https://luftfartstilsynet.no/droner/veiledning/spesifikk-kategori/ (visited on 22nd Jan. 2024).

[45] *Standard Scenario (STS)*. URL: https://www.easa.europa.eu/en/domains/civil-drones-rpas/specific-category-civil-drones/standard-scenario-sts (visited on 22nd Jan. 2024).

[46] Maryam Torabbeigi, Gino J. Lim and Seon Jin Kim. 'Drone Delivery Scheduling Optimization Considering Payload-induced Battery Consumption Rates'. In: *Journal of Intellegent and Robotic Systems* (2019). URL: https://doi.org/10.1007/s10846-019-01034-w.

[47] *unmanned aerial vehicle*. URL: https://www.thefreedictionary.com/Unmanned+Aerial+Vehicle (visited on 22nd Jan. 2024).

[48] *Veiledning*. URL: https://luftfartstilsynet.no/droner/veiledning/ (visited on 22nd Jan. 2024).

[49] Gary Vermaak and Adam Erickson. *Drone Delivery System- Where did it all begin?* URL: https://www.linkedin.com/pulse/drone-delivery-system-where-did-all-begin-dronelogisticsecosystem/ (visited on 18th Jan. 2024).

[50] *xcopterCalc - Multicopter Calculator*. URL: https://www.ecalc.ch/xcoptercalc.php (visited on 22nd Jan. 2024).

[51] Yunhong Yang, Xingzhong Xiong and Yuehao Yan. 'UAV Formation Trajectory Planning Algorithms: A Review'. In: *Drones* 7.1 (2023). ISSN: 2504-446X. DOI: 10.3390/drones7010062. URL: https://www.mdpi.com/2504-446X/7/1/62.

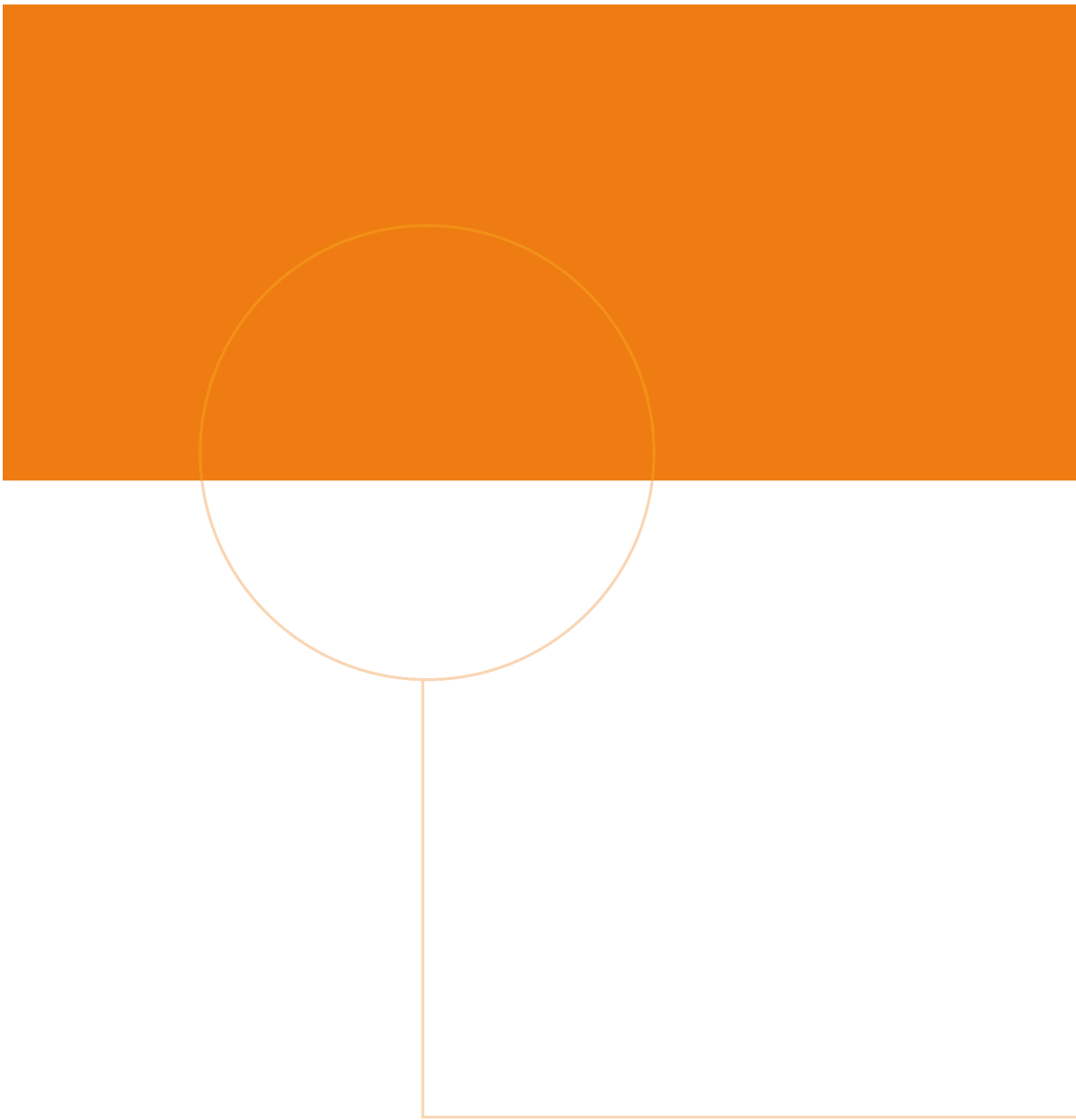

NTNU

Norwegian University of
Science and Technology